JOURNAL OF NEUROINFLAMMATION

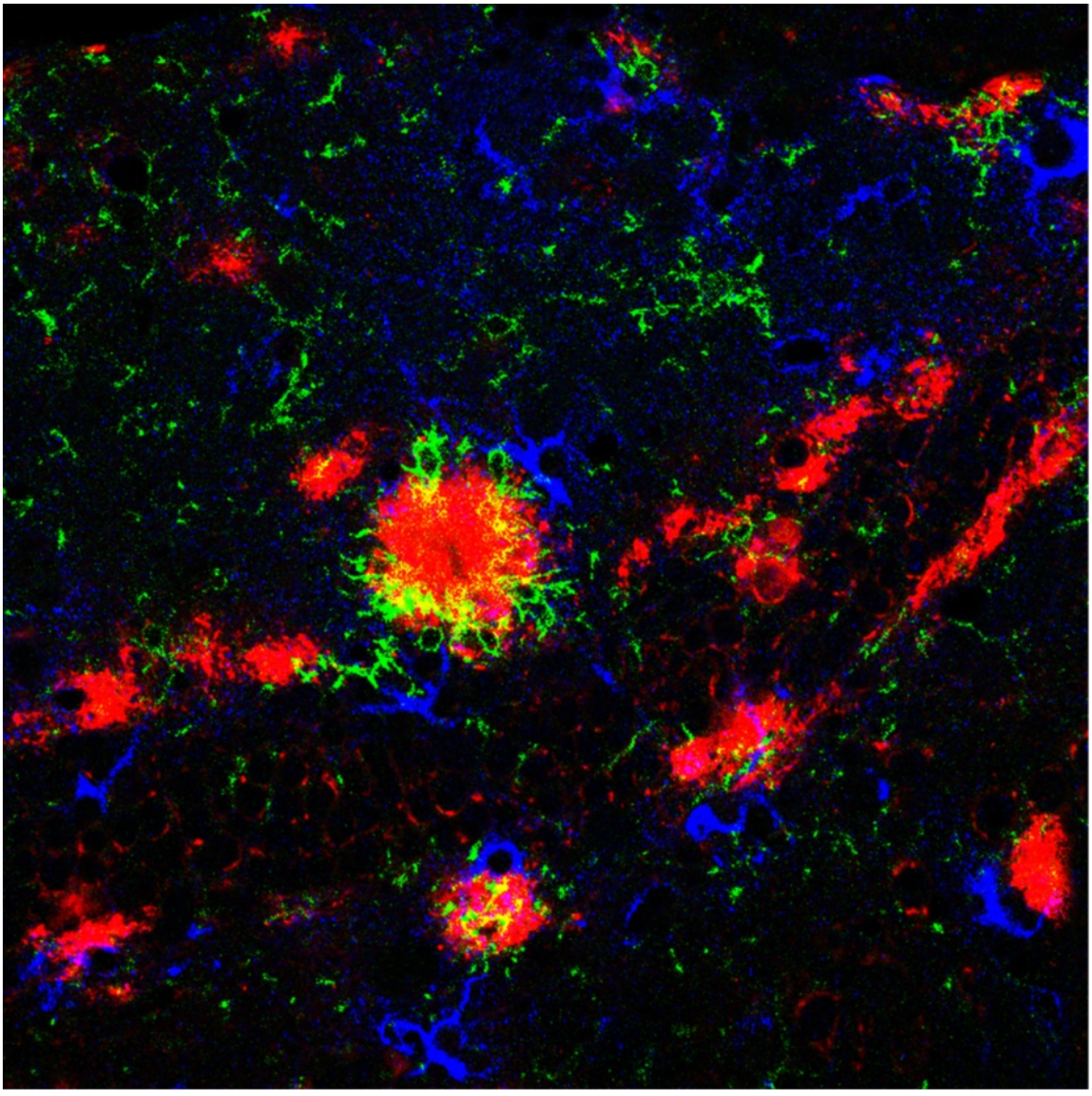

Cognitive and cerebrovascular improvements following kinin B_1 receptor blockade in Alzheimer's disease mice

Lacoste *et al.*

BioMed Central

Lacoste *et al. Journal of Neuroinflammation* 2013, **10**:57
http://www.jneuroinflammation.com/content/10/1/57

JOURNAL OF NEUROINFLAMMATION

RESEARCH Open Access

Cognitive and cerebrovascular improvements following kinin B_1 receptor blockade in Alzheimer's disease mice

Baptiste Lacoste[1], Xin-Kang Tong[1], Karim Lahjouji[2], Réjean Couture[2] and Edith Hamel[1*]

Abstract

Background: Recent evidence suggests that the inducible kinin B_1 receptor (B_1R) contributes to pathogenic neuroinflammation induced by amyloid-beta (Aβ) peptide. The present study aims at identifying the cellular distribution and potentially detrimental role of B_1R on cognitive and cerebrovascular functions in a mouse model of Alzheimer's disease (AD).

Methods: Transgenic mice overexpressing a mutated form of the human amyloid precursor protein ($APP_{Swe,Ind}$, line J20) were treated with a selective and brain penetrant B_1R antagonist (SSR240612, 10 mg/kg/day for 5 or 10 weeks) or vehicle. The impact of B_1R blockade was measured on i) spatial learning and memory performance in the Morris water maze, ii) cerebral blood flow (CBF) responses to sensory stimulation using laser Doppler flowmetry, and iii) reactivity of isolated cerebral arteries using online videomicroscopy. Aβ burden was quantified by ELISA and immunostaining, while other AD landmarks were measured by western blot and immunohistochemistry.

Results: B_1R protein levels were increased in APP mouse hippocampus and, prominently, in reactive astrocytes surrounding Aβ plaques. In APP mice, B_1R antagonism with SSR240612 improved spatial learning, memory and normalized protein levels of the memory-related early gene Egr-1 in the dentate gyrus of the hippocampus. B_1R antagonism restored sensory-evoked CBF responses, endothelium-dependent dilations, and normalized cerebrovascular protein levels of endothelial nitric oxide synthase and B_2R. In addition, SSR240612 reduced (approximately 50%) microglial, but not astroglial, activation, brain levels of soluble $Aβ_{1-42}$, diffuse and dense-core Aβ plaques, and it increased protein levels of the Aβ brain efflux transporter lipoprotein receptor-related protein-1 in cerebral microvessels.

Conclusion: These findings show a selective upregulation of astroglial B_1R in the APP mouse brain, and the capacity of the B_1R antagonist to abrogate amyloidosis, cerebrovascular and memory deficits. Collectively, these findings provide convincing evidence for a role of B_1R in AD pathogenesis.

Keywords: Brain kinins, Amyloid, Cerebral circulation, Neuroinflammation, Neuropeptide

Introduction

Alzheimer's disease (AD) is not only characterized by cognitive and cerebrovascular deficits [1], but also by neuroinflammation that may involve the kallikrein-kinin system (KKS) [2] known to be widely distributed in brain [3]. Kinins are proinflammatory and vasoactive peptides that act through the activation of two G protein-coupled receptors, denoted as B_1 and B_2 (B_1R and B_2R). Bradykinin (BK) and kallidin (Lys-BK) are the endogenous ligands for the constitutive B_2R whereas the C-terminal metabolites $desArg^9$-BK and Lys-$desArg^9$-BK are the preferential agonists of the inducible B_1R [4]. In the brain vasculature, BK dilates most cerebral arteries [5] through activation of B_2R and release of endothelial-derived nitric oxide (NO). BK also regulates blood–brain barrier (BBB) permeability [6]. Activation of the brain KKS occurs in hypertension [7], cerebral ischemia [8], head trauma [9] and diabetes [10], all

* Correspondence: edith.hamel@mcgill.ca
[1]Laboratory of Cerebrovascular Research, Montreal Neurological Institute, McGill University, 3801 University Street, Montréal, QC H3A 2B4, Canada
Full list of author information is available at the end of the article

known as important risk factors for developing AD with increased age [11].

In agreement with our preliminary studies [12,13], growing evidence also suggests a role for the KKS in AD [2], as reflected by the cleavage of high-molecular-weight kininogens observed in the cerebrospinal fluid (CSF) of AD patients [14]. Consistent with this observation, a single dose of BK infused into the rat hippocampus led to learning and memory deficits [15]. And, in rodents submitted to intracerebroventricular (i.c.v.) administration of $A\beta_{1-40}$, BK levels were increased in the CSF [16] and BK receptors density was upregulated in memory-related brain regions such as the prefrontal cortex and hippocampus [17,18]. Moreover, pharmacological or genetic blockade of the B_1R abrogated the cognitive deficits induced by a single i.c.v. injection of $A\beta_{1-40}$ in rodents [18], suggesting that B_1R could represent a target for AD therapy. Other reports indicated that B_1R blockade protects mice from focal brain injury by controlling BBB leakage [19], a disruption evidenced in the AD brain [20].

However, a critical role for kinins in AD cognitive and cerebrovascular deficits has never been confirmed in a clinically relevant transgenic mouse model that recapitulates a wide array of AD landmarks (cerebrovascular, cognitive, neuroinflammation and amyloid pathologies), such as mice that overproduce chronically Aβ peptide through transgene expression of familial AD-related mutated human amyloid precursor protein (hAPP) [21]. Here, we sought to investigate whether B_1R upregulation could contribute to neuronal, glial, and cerebrovascular dysfunctions in mice overexpressing the $hAPP_{Swe,Ind}$ mutations [22] (APP mice). In addition to providing the first description of B_1R immunoreactivity in the APP mouse forebrain, our data demonstrate that pharmacological blockade of the B_1R counters the cerebrovascular, cognitive and anatomopathological deficits in adult APP mice with a fully developed pathology.

Material and methods

All experimental procedures were conducted in accordance with the guidelines of the Canadian Council on Animal Care, and the protocols were approved by the Animal Care Committee at McGill University. In order to ensure the best reproducibility, experiments for each treatment cohort were conducted independently (at six-month intervals). For a rigorous interpretation of data within each cohort (for example immunohistochemistry, ELISA and western blotting), brain extracts and sections from the four experimental groups (see below) were processed simultaneously.

Reagents and antibodies

For selective blockade of the B_1R, the non-peptide, brain penetrant B_1R antagonist SSR240612 [(2*R*)-2-[((3*R*)-3-(1,3-benzodioxol-5-yl)-3-{[(6-methoxy-2-naphthyl)sulfonyl]amino}propanoyl)amino]-3-(4-{[2*R*,6*S*)-2,6-dimethylpiperidinyl]methyl}phenyl)-*N*-isopropyl-*N*-methylpropanamide hydrochloride] was kindly provided by Sanofi-Aventis (Montpellier, France) [23]. SSR240612 is a stable and highly selective blocker of des-Arg^9BK binding at B_1R with a K_i of 0.48 nM, which was previously tested in man for neuropathic pain [24].

Detection of BK receptor proteins was performed by western blot and immunohistochemistry using selective anti-B_1R and -B_2R antibodies raised in rabbits (Biotechnology Research Institute, Montréal, QC, Canada) against a conserved amino acid sequence from B_1R and B_2R proteins of mouse and rat [25]. The epitopes used contained 15 amino acids localized in the C-terminal region of B_1R (VFAGRLLKTRVLGTL) and 15 amino acids localized in the second extracellular domain of B_2R (TIANNFDW VFGEVLC). Care was taken to avoid sequences with similarity to related mammalian proteins, including the opposite receptor. Two negative controls were run for each antibody: the pre-immune serum and the receptor-specific immunogenic peptide; both completely prevented any immunostaining. Specificity of our B_1R antibody was further determined using mouse kidney extracts, an organ particularly rich in constitutive B_1R [26], from wild-type (WT) and B_1R knockout (KO) mice (kindly provided by Dr. Jean-Pierre Girolami, INSERM U1048, Université Paul Sabatier, Toulouse, France). Western blotting confirmed that the anti-B_1R antibody recognized a single band at 37 kDa in the kidney of WT mice, which was absent from B_1R KO mice kidney extracts (Figure 1A).

The other reagents were as follows: serotonin (5-HT) and acetylcholine (ACh) from Sigma-Aldrich (St Louis, MO, USA), BK from American Peptide (Sunnyvale, CA, USA). Antibodies were rabbit anti-beta-secretase-1 (BACE, M-83, Santa Cruz Biotechnology, Santa Cruz, CA, USA), -glial fibrillary acidic protein (GFAP, Dako, Glostrup, Denmark), -ionized calcium-binding adaptor molecule 1 (Iba1, Wako Chemicals USA, Inc., Richmond, VA, USA), -early growth response protein 1 (Egr-1 or Zif268, C-19, Santa Cruz Biotechnology,), and -matrix metallopeptidase 9 (MMP9, Millipore, Chemicon, Billerica, MA, USA), guinea pig anti-GFAP (Synaptic Systems, Goettingen, Germany), mouse anti-endothelial nitric oxide synthase (eNOS, BD Transduction Laboratories, Mississauga, ON, Canada), -amyloid-beta $(A\beta)_{1-16}$ (6E10, Covance, Princeton, NJ, USA), -β-actin (Sigma-Aldrich), -dynein (Santa Cruz Biotechnology), rat anti-cluster of differentiation molecule 11b (CD11b, Serotec, Raleigh, NC, Canada), and goat anti-lipoprotein receptor-related protein 1 (LRP-1, N-20, Santa Cruz Biotechnology). Biotinylated, cyanin Cy2-, Cy3- or Cy5- and horseradish peroxidase-conjugated secondary antibodies were from Vector Laboratories (Burlingame, CA, USA) and Jackson

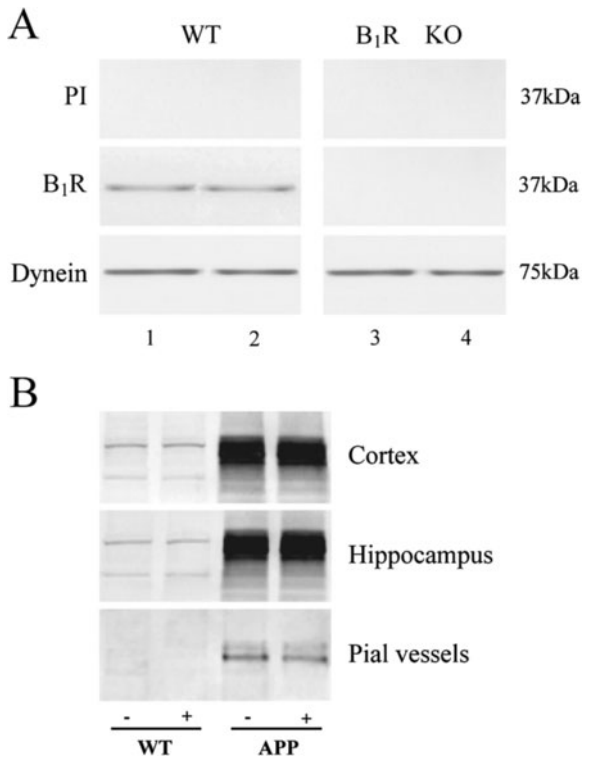

Figure 1 Experimental controls. (A) Western-blot analysis of bradykinin receptor 1 (B_1R) pre-immune (PI) and anti-serum on kidney extracts from two wild-type (WT; 1,2) and two B_1R knockout (KO; 3,4) mice. The anti-B_1R antibody recognized a single band at the expected molecular weight (37 kDa), which was absent in B_1R KO mice or in the presence of pre-immune serum. Dynein was used as standard. **(B)** Transgenic amyloid precursor protein (APP) mice featured increased expression of APP in both brain and pial vessels extracts, as measured by western blot. APP protein levels were not affected by vehicle (–) or treatment (+).

Laboratories (West Grove, PA, USA), respectively. Avidin-biotin complex (ABC), 3,3′-diaminobenzidine (DAB) and slate gray (SG) reagent kits were from Vector Laboratories. ECL Plus kit for enhanced chemiluminescence was from Amersham (Mississauga, ON, Canada).

Animals and treatment

We used heterozygous transgenic adult C57BL/6 mice (10 months old) that express the human amyloid precursor protein (hAPP) carrying the Swedish (K670N, M671L) and Indiana (V717F) familial AD mutations directed by the platelet-derived growth factor (PDGF) β-chain promoter (APP mice, J20 line) [22] and age-matched WT littermates, with approximately equal numbers of females and males. None of the parameters measured in the present study were affected by gender. We selected the J20 mice because at 10 months of age they display the full spectrum of cerebrovascular, cognitive, neuroinflammation and amyloid pathologies [22,27,28], hence allowing therapeutic rescue rather than preventive intervention, which we believe has high relevance for AD patients. Two cohorts (n ≥48 each) were divided in four groups (WT-vehicle, WT-treated, APP-vehicle, APP-treated) and treated with SSR240612 for periods of 5 or 10 weeks. Due to compound solubility and minipump limitations, the maximal administrable dose was 10 mg/kg/day. As promising, yet incomplete beneficial effects were observed after 5 weeks of treatment, a second cohort received SSR240612 during 10 weeks. SSR240612 was diluted at 215 mM in 40% DMSO and 60% sterile saline (NaCl) added in this sequence. SSR240612 (10 mg/kg/day) and vehicle (40% DMSO, 60% NaCl) were delivered (0.11 μl/hr, 5 weeks) through osmotic minipumps (model 1004, Alzet™, Durect Corporation, Cupertino, CA, USA), which were implanted subcutaneously under isoflurane anesthesia. For the treatment of 10 weeks, minipumps were removed after 5 weeks and replaced by new ones for an additional 5-week period. Treatment did not affect APP transgene expression in brain or vascular tissues (Figure 1B).

Morris water maze

The ability of mice to learn and remember the location of a platform in a predefined (target) quadrant in a circular pool filled with opaque water (17°C) using visuo-spatial cues was tested during eight consecutive days (three days of visible platform training followed by five days of hidden platform trials), as described elsewhere [29]. Platform location and visual cues distribution were altered between the visible and hidden platform testings. Twenty-four hours after the last hidden platform trial, on day 9, mice were submitted to a 60-sec probe trial (platform removed). Visual acuity and locomotor ability were comparable between all groups, as assessed during the visible platform testing. All experiments were started at the same time every day. Daily escape latencies to the platform, percentage of time spent and distance traveled in the target quadrant during the probe trial, along with swim speed, were collected with the 2020 Plus tracking system and analyzed with the Water 2020 software (HVS Image, Buckingham, UK).

Laser Doppler flowmetry

Laser Doppler flowmetry measurements (Transonic Systems Inc., Ithica, NY, USA) of evoked cerebral blood flow (CBF) in response to sensory stimulation were carried out one week following the Morris water maze in anesthetized mice (n = 4 to 6, ketamine 80 mg/kg intraperitoneally; Wyeth, St-Laurent, QC, Canada) fixed in a stereotaxic frame [28]. CBF was recorded over the contralateral somatosensory cortex before, during and after unilateral stimulation of the right whiskers (20 sec at 8 to 10 Hz). Six recordings were acquired every 30 to 40 sec and averaged for each mouse. The entire procedure lasted less than 30 min, a time window when all

physiological parameters remain stable [30]. Cortical CBF changes were expressed as percentage increase relative to baseline.

Vascular and brain tissue collection

Mice were killed by cervical dislocation and middle cerebral artery (MCA) segments immediately tested in vascular reactivity studies. For immunohistochemistry (IHC), western blot (WB) and ELISA studies, mice were exsanguinated by intracardiac perfusion of sterile 0.9% NaCl under deep sodium pentobarbital anesthesia. Vessels of the circle of Willis and their branches free of pial membrane along with cortex and hippocampus of one hemibrain were collected, snap-frozen on dry ice and stored (−80°C). The other hemibrain was fixed by overnight immersion in 4% paraformaldehyde (PFA) in 0.1 M phosphate-buffered saline (pH 7.4), cryoprotected, frozen in isopentane (−45°C) and stored (−80°C) until cutting into 25 μm-thick free-floating coronal sections using a freezing microtome.

Vascular reactivity

In order to assess the impact of B_1R blockade on the reactivity of cerebral vessels, isolated, pressurized and submaximally precontracted (5-HT, 2.10^{-7} M) MCA segments (diameter 40 to 70 μm) from WT and APP mice were tested for dilatation to ACh (10^{-10} to 10^{-5} M) and BK (10^{-10} to 10^{-5} M) using online videomicroscopy [31]. Percentage changes in vessel diameter from pre-constricted tone were plotted as a function of agonist concentration. The maximal response (EAmax) and the concentration eliciting half of EAmax (EC_{50} value, or $pD_2 = -[\log EC_{50}]$), were generated by the GraphPad Prism software (version 4, San Diego, CA, USA) and used to evaluate agonist efficacy and potency, respectively.

Immuno- and histochemical staining

Sections were pretreated with 3% H_2O_2 (20 min) and incubated overnight at room temperature (RT) with either rabbit anti-B_1R (1:1500) or -Egr-1 (1:250) antibodies diluted in a blocking buffer, followed by biotinylated anti-rabbit IgGs and the ABC kit; labeling was revealed with 0.05% DAB (B_1R) or SG (Egr-1). To study basal Egr-1 expression levels and avoid task-induced changes [32], Egr-1 immunohistochemistry was done on animals sacrificed three days post-water maze. For detection of dense core amyloid plaques, sections from APP mice were stained with 1% thioflavin-S (8 min). Sections from all groups were incubated with rabbit anti-GFAP (1:400), -Iba1 (1:300), mouse anti-$A\beta_{1-16}$ (1:1000), or goat anti-LRP-1 (1:250), followed by species-specific Cy2- (GFAP and Iba1) or Cy3- (LRP-1) conjugated secondary antibodies (1:300) for the detection of activated astrocytes, microglia, diffuse and dense-core Aβ plaques, or LRP-1, respectively. Sections were observed under a Leitz Aristoplan microscope using bright field or an FITC filter and epifluorescence (Leica, Montréal, QC, Canada) and digital pictures were acquired with a digital camera (Coolpix 4500; Nikon, Tokyo, Japan). For double immunofluorescence, sections were simultaneously incubated with a rabbit anti-B_1R antibody and either a guinea pig anti-GFAP, rat anti-CD11b, or mouse anti-$A\beta_{1-16}$ antibody, followed by donkey anti-rabbit Cy3- and species-specific Cy2-conjugated IgGs. Triple immunolabeling was also performed by co-incubating sections with rabbit anti-B_1R (with Cy5 secondary), rat anti-CD11b (Cy2) and mouse anti-$A\beta_{1-16}$ (Cy3) antibodies. Sections were observed and images acquired under a Zeiss LSM 510 laser scanning confocal microscope (Carl Zeiss Ltd., Toronto, ON, Canada) equipped with appropriate filters.

Staining quantification

Digital images (two to three sections/mouse, n = 4 to 6 mice) taken under the same conditions were analyzed with MetaMorph (6.1r3, Universal Imaging, Downingtown, PA, USA). The areas of interest (somatosensory/cingulate cortex, dorsal hippocampus) containing thioflavin S-, 6E10-, GFAP-, Iba1- and LRP-1-positive elements were manually outlined in MetaMorph on low-power digital pictures (as exemplified in Figure 1A by dashed lines), whereas high-power images of the hippocampus were used for quantification of Egr-1 immunostaining. For microglial proliferation, the numbers of Iba-1-positive cell bodies were manually counted on digital pictures (two pictures from cortex, one from hippocampus including the dentate gyrus (DG), from three immunostained sections per mouse). The area occupied by Iba1- and GFAP-positive cells was also quantified and expressed as a percentage of surface occupied by labeling within the delineated areas of interest. Since clusters of activated microglial emit a stronger immunofluorescence signal, the maximal intensity of Iba-1 labeling was measured by dividing the maximal gray value of staining by the total gray value of the delineated area. The area occupied by thioflavin S- and 6E10-positive plaques, as well as by LRP-1 -positive cells was also measured, together with the intensity (total gray value) of LRP-1 immunofluorescence. For better LRP-1 staining illustration, colors on micrographs were inverted and desaturated. Quantification of Egr-1 immunoreactivity in the hippocampus included both the total gray value in CA1-CA2 areas and the number of positive nuclei in the DG.

Enzyme-linked immunosorbent assay (ELISA)

Levels of soluble $A\beta_{1-40}$ and $A\beta_{1-42}$ were measured in homogenized hemibrains from APP mice (n = 4 to 5)

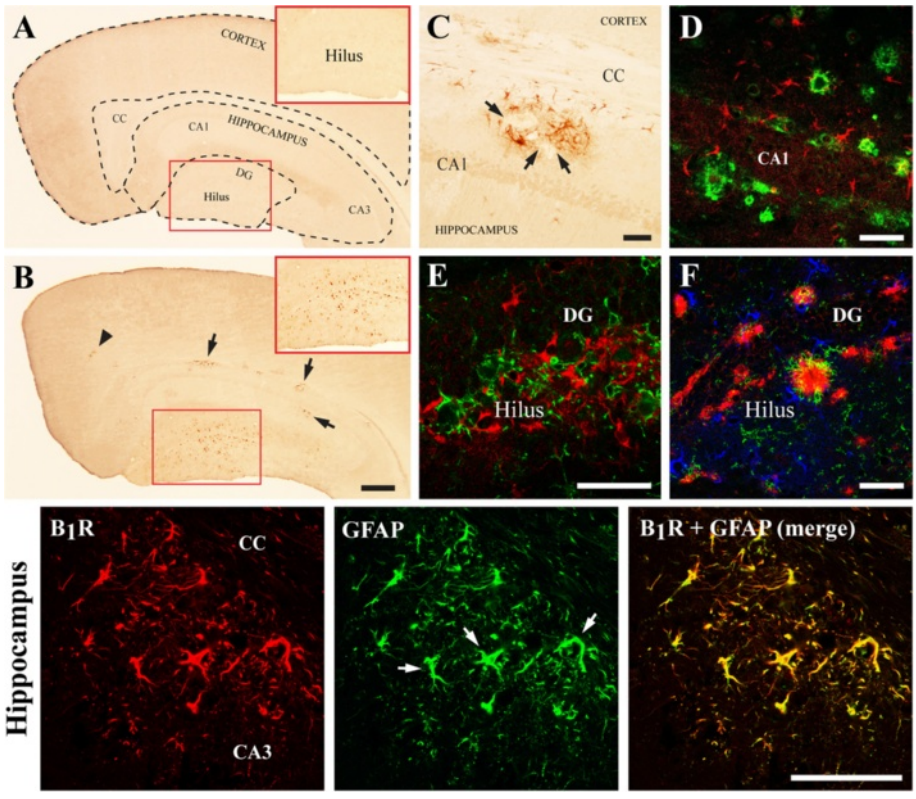

Figure 2 Distribution of B_1R in WT and APP mouse forebrain: co-localization with reactive astrocytes. (A,B) Single B_1R immunohistochemical labeling (revealed with DAB, brown precipitate) in the somatosensory cortex and dorsal hippocampus of WT **(A)** and APP **(B)** mice. B_1R were upregulated in the APP mouse brain (insets: high magnification of dentate gyrus (DG)). **(C-F)** High magnification of B_1R immunolabeling in APP mice hippocampus. **(C)** Single B_1R immunoreactive cells (DAB staining) surrounding unlabeled parenchymal zones (arrows). **(D)** Double immunofluorescence of B_1R-positive cells (red) intermingled around small Aβ plaques (green). (E) Double immunofluorescence of B_1R (red) and CD11b (green) showed that they label distinct cellular elements. **(F)** Triple immunofluorescence of B_1R (blue), Aβ (red) and CD11b (green) showed that B_1R-positive cells surround the outside rim of Aβ plaques, and are distinct from CD11b-positive microglial cells. Lower panel: double immunofluorescence of B_1R (red) and GFAP (green) in hippocampus of APP mice confirmed that B_1R immunoreactivity is predominantly localized in astroglial cells. DG, dentate gyrus; CC, corpus callosum. Scale bars: 100 μm, except in B: 300 μm. N = 3 to 8/group. Aβ, amyloid-beta; APP, amyloid precursor protein; B_1R, bradykinin receptor 1; CD11b, cluster of differentiation molecule 11b; GFAP, glial fibrillary acidic protein; WT, wild-type.

using ELISA kits (BioSource International, Camarillo, CA, USA), as described before [28]. Data were collected as optical density values in the tissue supernatants and expressed as a percentage of untreated APP mice.

Western blot

For protein quantification (n = 5 to 6 mice/group), vessels were homogenized in Laemmli buffer and cortex and hippocampus in a lysis buffer [31]. In brief, extracts were protein assayed, loaded (5 to 50 μg) in 10% SDS-polyacrylamide gels, separated by electrophoresis and transferred to nitrocellulose membranes. Membranes were incubated (1 h, RT) in a blocking buffer containing 5% skim milk and then (overnight, 4°C) with either rabbit anti-B_1R (1:500), -B_2R (1:500), -BACE (1:1000), -MMP9 (1:1000), or mouse anti-$A\beta_{1\text{-}16}$ (1:1000), -eNOS (1:1000), -β-actin (1:10000), or -dynein (1:25000). Membranes were further incubated (1 h, RT) with horseradish peroxidase-conjugated secondary antibodies (1:2000) and proteins visualized by chemiluminescence (ECL Plus kit) using a phosphorImager (Scanner STORM 860; GE Healthcare, Piscataway, NJ, USA), followed by densitometric quantification (ImageQuant 5.0, Molecular Dynamics, Sunnyvale, CA, USA).

Statistical analysis

All data are means ± SEM and were analyzed with GraphPad 4 (San Diego, CA, USA) or Statistica 10 (StatSoft, Tulsa, OK, USA) software. Two-group comparisons (effects of treatment on amyloidosis) were analyzed by unpaired Student's *t* tests. Four-group comparisons were analyzed using two-way analysis of variance (ANOVA, genotype and treatment as factors) followed by a Newman-Keuls post hoc test when the interaction or at least one factor was significant. $P < 0.05$ was considered significant. Except for vascular reactivity, anatomical and western blot

studies, experiments were conducted blind to the mouse identity. The relationships between amyloid burden and cognitive performance or LRP-1 immunoreactivity were assessed by plotting the averages of Aβ plaque load (percentage area) from thioflavin-S and 6E10 stainings with those of the cognitive score (percentage of time and percentage of distance spent in the target quadrant) or LRP-1 immunostaining (percentage of intensity or percentage of occupied area) in the cortex, hippocampus and DG in five non-treated and five treated APP mice from the 10-week treatment cohort.

Results

Upregulation of B_1R in the APP mouse brain

Since localization and expression of BK receptors in the rodent brain has been described by autoradiography of radioligand binding sites and by western blot [9,17,18], we first investigated the immunohistochemical distribution of the B_1R protein in WT and APP mice using highly selective primary antibodies. B_1R immunoreactivity was very low to absent in the cortex and hippocampus of WT mice (Figure 2A), with only a faint, barely detectable staining in the DG (Figure 2A, inset). In APP mice, B_1R immunostaining was increased in the hippocampus (Figure 2B, arrows), primarily in the DG that displayed abundant immunopositive cells in the hilus region (Figure 2B, inset), whereas only few B_1R-positive cells were found in cortex (Figure 2B, arrowhead). In APP hippocampus (Figure 2B, C), B_1R-positive clusters contained glia-shaped cells with hypertrophied processes surrounding empty parenchymal zones characteristic of amyloid deposition, as confirmed in high-power micrographs of double immunofluorescence for B_1R and $A\beta_{1\text{-}16}$ (Figure 2D; see also 2F). The upregulated B_1R immunoreactivity did not co-localize with the CD11b marker for activated microglia (Figure 2E,F), but with the typical astroglial GFAP marker (Figure 2, bottom). B_1R-positive astrocytes in APP mice displayed enhanced GFAP immunostaining, hypertrophic processes and soma (Figure 2, bottom, white arrows). No B_1R-positive blood vessels were detected in pia or parenchyma of the mouse brain, in accordance with B_1R not mediating BK-mediated vasomotor responses [33].

Improvement of learning and memory following B_1R blockade in APP mice

In order to investigate whether B_1R blockade could alter behavioral outcome in APP mice, cognitive performances were assessed in the Morris water maze paradigm in our two cohorts of mice. Although APP mice were slightly slower than WT mice in reaching the visible platform at specific time points, they had no visual or motor deficit and all groups performed similarly on day 3 (Figure 3A,B). In contrast, both learning and memory were significantly impaired in APP mice compared with WT littermates. APP mice displayed increased latencies to reach the hidden platforms (Figure 3A,B, left) and reduced time spent and distance traveled in the target quadrant (−50%; P <0.01) during the probe trial (Figure 3A,B, right) although swim speeds were similar among all groups (data not shown). Both 5 and 10 weeks of SSR240612 treatment greatly improved learning and memory performances in APP mice, without any effect on WT mice. Recovery was comparable after 5 or 10 weeks of drug delivery.

Normalization of Egr-1 protein levels in the DG of the hippocampus in SSR240612-treated APP mice

We then studied Egr-1 (Zif268) protein levels in hippocampus, a transcription factor related to synaptic activity [34], and required for memory induction and consolidation [35]. Basal expression of Egr-1 is reduced in APP mice [30,36], and upregulated in adult APP mice with pharmacologically restored memory [30]. We confirmed a drastic reduction (50 to 70%, P <0.001) of Egr-1 staining intensity in the CA1-CA2 region (Figure 4A,B) of the hippocampus in APP mice. However, despite significant improvement in memory after SSR240612, no beneficial effect of treatment was evidenced on Egr-1 expression in this region. In contrast, in addition to a higher Egr-1 staining intensity readily detectable in the hilus of the DG of treated compared to untreated APP mice (Figure 4C), a partial but significant recovery (+25%; P <0.05) in the reduced number (−60%; P <0.001) of Egr-1-positive nuclei was also observed following 10, but not 5 weeks of SSR240612 treatment (Figure 4C).

B_1R blockade reduced soluble $A\beta_{1-42}$ species and amyloidosis

As expected [22], transgenic APP mice featured high brain levels of soluble Aβ peptide, as measured by ELISA ($A\beta_{1\text{-}40}$ and $A\beta_{1\text{-}42,}$ Figure 5A,B), and of aggregated and deposited Aβ species as measured by thioflavin-S staining (dense-core Aβ plaques, Figure 5C) and 6E10 immunohistochemistry (total amyloid, Figure 5D). Following short- and long-term SSR240612 administration, levels of soluble $A\beta_{1\text{-}42}$ species were selectively decreased in hemibrains (Figure 5A,B), and mature and diffuse Aβ plaque loads were significantly reduced in the somatosensory/cingulate cortex and dorsal hippocampus (Figure 5C,D). Both the 5- and 10-week treatments exerted reducing effects on amyloidosis, but the total Aβ plaque load in neocortex was significantly decreased only after the longer treatment (Figure 5D).

B_1R blockade, lipoprotein receptor-related protein-1 (LRP-1) and matrix metallopeptidase 9 (MMP9)

Since brain Aβ homeostasis is highly regulated by Aβ clearance at the BBB by LRP-1 [37,38], we investigated whether SSR240612 treatment could impact on this Aβ efflux system. WT and APP mice showed few LRP-1-

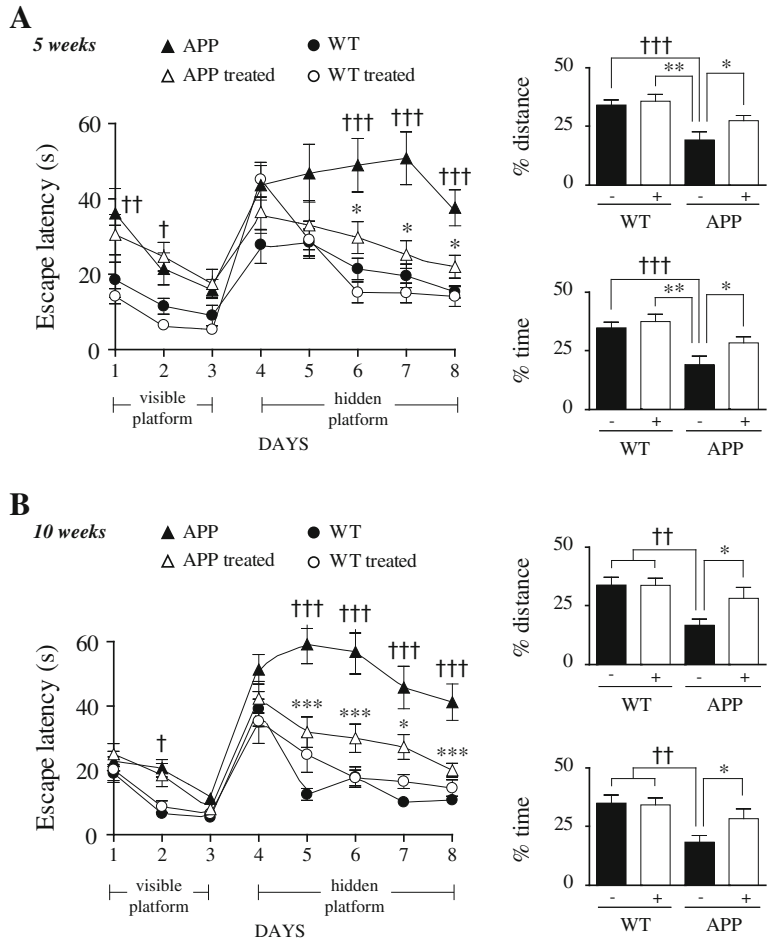

Figure 3 SSR240612 treatment improved spatial learning and memory in APP mice after 5 (A) and 10 weeks (B) of treatment. In the Morris water maze, APP mice (▲) displayed impaired learning in the hidden-platform testing (left), and memory deficit in the probe trial (platform removed) performed on day 9 (right) compared to both non-treated WT (●) and treated WT (○) controls. SSR240612 partly rescued these deficits in treated APP mice (**Δ**) that did not statistically differ from WT control groups. SSR240612 had no effect in WT. APP mice did not feature motor or visual deficits as shown by their ability to reach the visible platform as effectively as WT by day 3. Error bars represent SEM. **P* <0.05; **, ††*P* <0.01; ***, †††*P* <0.001. Two-way ANOVA followed by Newman-Keuls post hoc test (†: APP vs. WT, *: APP vs. APP treated). N = 10 to 15/group. APP, amyloid precursor protein; WT, wild-type.

immunoreactive neurons in cortex and hippocampus, with immunoreactive vessels being present along the cortical surface and throughout the hippocampus (Figure 6A). SSR240612 treatment decreased LRP-1 immunoreactivity in brain parenchyma and microvessels of treated WT mice. In contrast, 5 and 10 weeks of SSR240612 treatment significantly increased (approximately 30 to 40%) LRP-1-labeled area and intensity in APP mice depending on the brain region (Figure 6A). Neuronal LRP-1, in contrast, remained unchanged after treatment, compatible with neuronal LRP-1 expression being independent of amyloidosis in AD mice [39]. As MMP9 is involved in both BBB integrity and Aβ clearance [40-43], its protein levels were also measured. Following 10 but not 5 weeks of drug administration, a 50 to 60% increase (*P* <0.01) in MMP9 protein levels was evidenced in the cortex and hippocampus of WT and APP mice (Figure 6B), whereas those of the Aβ-generating enzyme BACE-1 were not altered (Figure 6B), the latter supporting that SSR240612 acted beyond Aβ synthesis.

SSR240612 reduced microglial, but not astroglial, activation in APP mice

Knowing that neuroinflammation mediated by astrocytes and microglia is induced in AD [44], as replicated in the brain of APP mice by the enhanced GFAP (astrocytes, Figure 7A) and Iba1 (microglia, Figure 7B) immunofluorescence, we sought to investigate whether the SSR240612-induced decrease in amyloidosis would be accompanied by a reduction in activated glial cells. Upregulated GFAP immunostaining in APP mice occurred primarily as

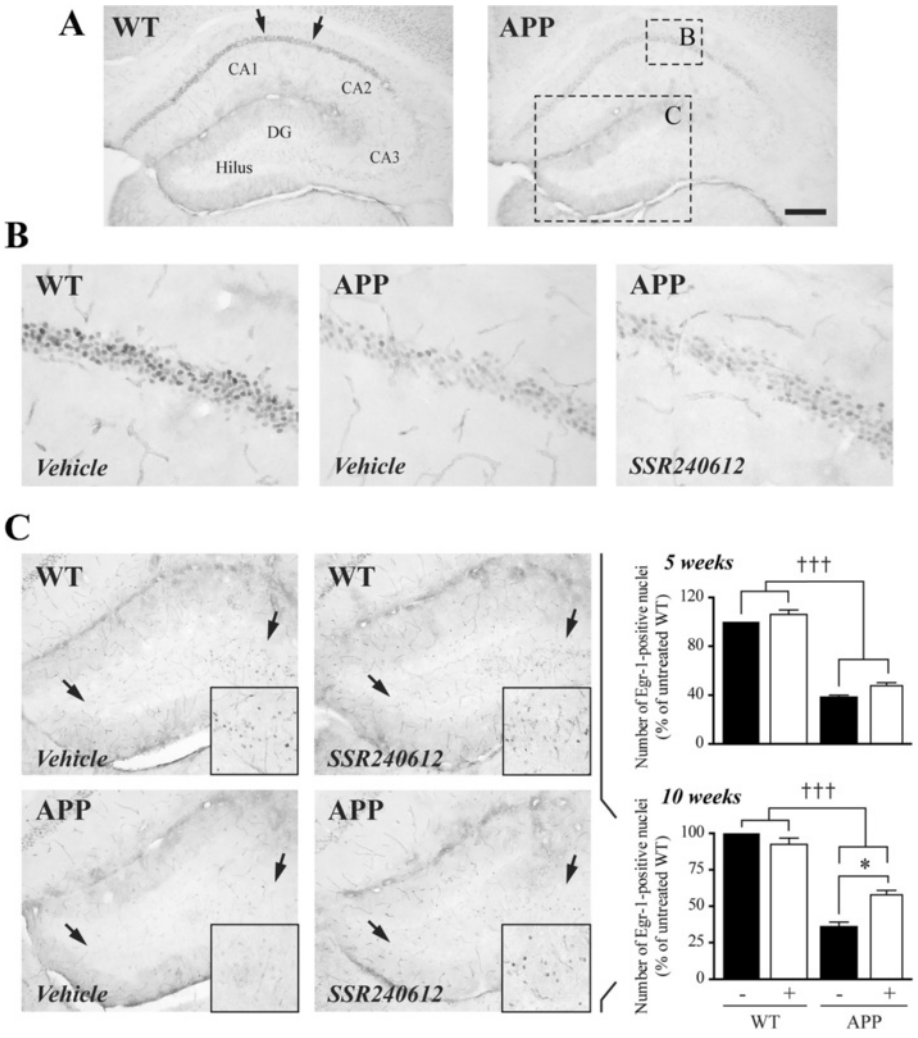

Figure 4 Decreased basal Egr-1 protein levels in APP mice hippocampus are partially restored in the dentate gyrus after 10 weeks of SSR240612 delivery. (A) Immunohistochemistry in the dorsal hippocampus revealed a drastic reduction in Egr-1 staining intensity (total gray value) in the CA1-CA2 fields **(B)**, and in the number of Egr-1-positive nuclei in dentate gyrus DG, **(C)** of APP mice. SSR240612 treatment had no effect on Egr-1 expression in CA1 **(B)**. **(C)** In contrast, following 10 weeks of delivery, SSR240612 partially countered Egr-1 reduction in the DG of APP mice. Quantified areas are delineated in A (arrows in WT; dashed boxes in APP) and magnified in B and C. See insets for higher magnifications. Scale bar: 300 μm. **P* <0.05; ††*P* <0.01; †††*P* <0.001 (†: vs. WT; *: non-treated APP vs. treated APP). Two-way ANOVA followed by Newman-Keuls post hoc test. N = 5/group. APP, amyloid precursor protein; Egr-1, early growth response protein 1; WT, wild-type.

patchy islands (Figure 7A, insets) reminiscent of Aβ deposits in neocortex and hippocampus, but SSR240612 treatment (5 and 10 weeks) did not lessen the extent of astroglial activation (Figure 7A). In contrast, the increase in microglial Iba1-positive area and, mainly, Iba1 staining intensity in APP brain were significantly reduced following SSR240612 treatment (Figure 7B). The patchy areas associated with plaques (Figure 7B, insets) were much less apparent in all regions after 10 weeks of drug delivery. Hippocampus, including the DG, was more responsive to treatment than cortical areas. In contrast, microglial proliferation was not affected by genotype or by treatment, as evidenced by the unchanged Iba1-positive cells number in all conditions (Table 1).

Improvement of cerebrovascular function following B_1R antagonism

Cerebral blood flow

The CBF response evoked by increased neuronal activity is impaired in APP mice [28,45], as found here in our two cohorts of adult mice compared to their respective WT controls (5 weeks: -65%, P <0.001; 10 weeks: -41%, P <0.05). SSR240612 treatment significantly ameliorated these sensory-evoked hemodynamic responses (+41% and +36%; respectively for 5 and 10 weeks, P <0.05), as

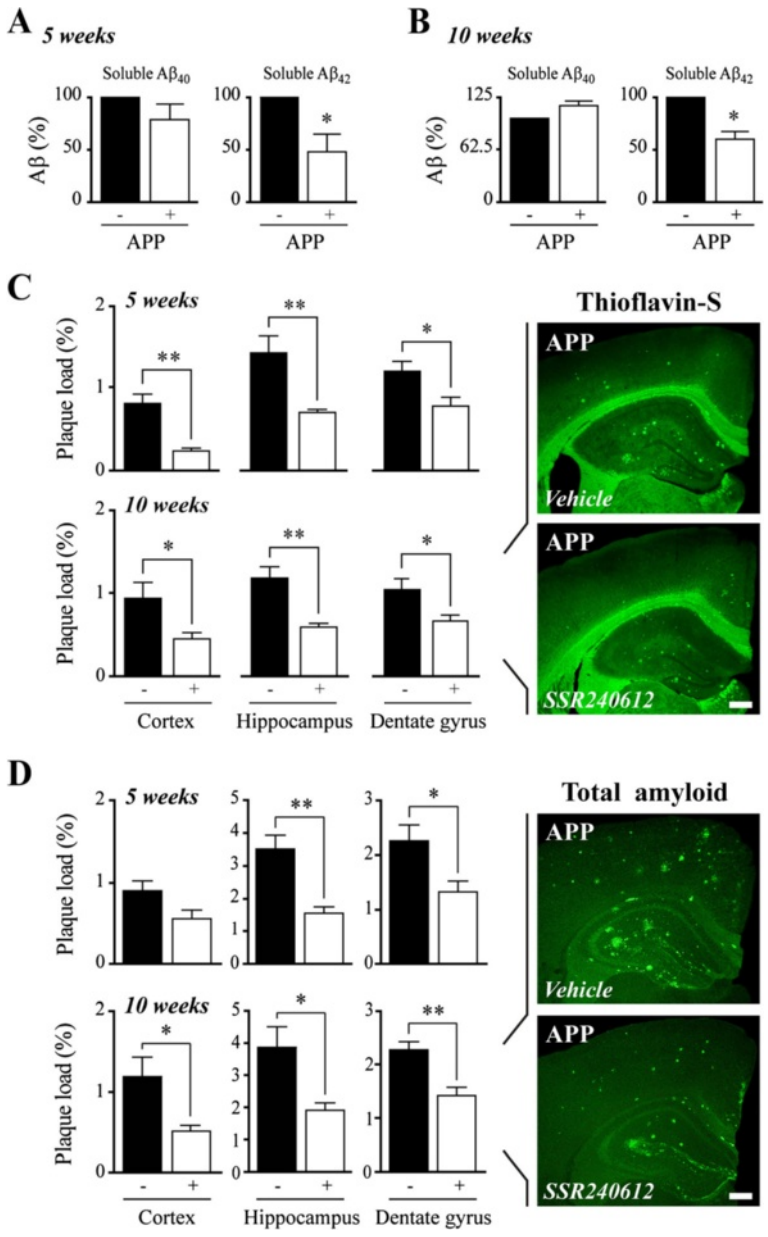

Figure 5 SSR240612 reduced soluble $A\beta_{1-42}$ in hemibrains and Aβ plaque load in cortex and hippocampus. (A,B) Levels of soluble $A\beta_{1-42}$ were significantly reduced in the brain of APP mice after 5 **(A)** and 10 weeks **(B)** of B_1R blockade, as observed by ELISA. **(C,D)** Following SSR240612 treatment, thioflavin-S staining **(C)** and 6E10 immunohistochemistry **(D)** revealed a significant reduction in the surface area occupied by mature and diffuse Aβ plaques (plaque load) in both cortex and hippocampus (including the dentate gyrus). Error bars represent SEM. *P <0.05; **P <0.01, Student's t test. N = 4 to 6/group. Aβ, amyloid-beta; APP, amyloid precursor protein; B_1R, bradykinin receptor 1.

illustrated in Figure 8A for the 5 weeks of treatment cohort. There was no added benefit with the longer treatment.

Cerebrovascular reactivity

In APP mice, the cerebrovascular contractile capacity is unaltered up to 21 months of age, whereas dilatory function is impaired early [28,31,46]. Hence, we tested whether SSR240612 could improve the dilatory deficits. As expected, arteries from adult APP mice featured significantly decreased dilatory responses to ACh over a wide range of concentrations, with a 40 to 50% reduction in EAmax compared to WT and no change in affinity, mean pD_2 values being comparable (Figure 8B, Table 2). Following 5 or 10 weeks of SSR240612 administration, impaired cerebrovascular dilation to ACh in APP mice was completely normalized, with dose-dependent and maximal responses, as well as agonist potencies, being

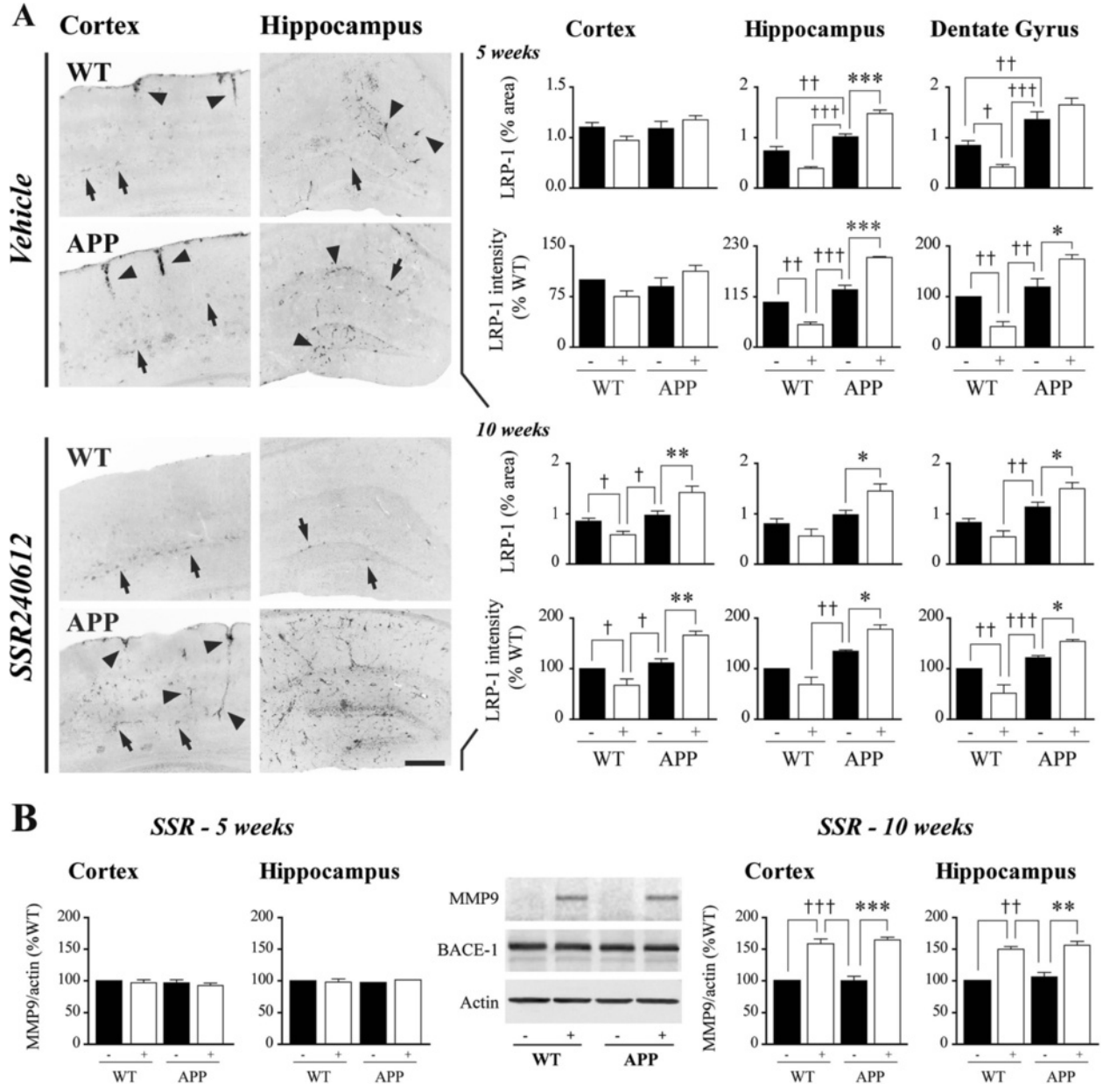

Figure 6 Effects of B_1R blockade on brain and vascular LRP-1 and brain MMP9. (A) SSR240612 increased LRP-1 protein levels in the APP mouse brain. Vascular (arrowheads), but not neuronal (arrows), lipoprotein receptor-related protein 1 (LRP-1) immunolabeling (left) was altered by genotype and/or treatment. LRP-1 immunostaining associated to brain vessels was decreased in treated WT mice and slightly increased in untreated APP mice. SSR240612 further increased LRP-1 vascular immunoreactivity in APP mice, in the hippocampus after 5, and in both cortex and hippocampus after 10 weeks of drug administration. Scale bar: 300 μm. **(B)** Additionally, after 10 but not 5 weeks of drug administration, the protein levels of MMP9 were increased by 50 to 60% in the brain of treated animals. Blots images illustrate the hippocampus from the 10 weeks of treatment cohort. Error bars represent SEM. *, †P <0.05; **, ††P <0.01; ***, †††P <0.001 (†: vs. WT; *: non-treated APP vs. treated APP). Two-way ANOVA followed by Newman-Keuls post hoc test. N = 5 to 6/group. APP, amyloid precursor protein; B_1R, bradykinin receptor 1; MMP9, matrix metallopeptidase 9; WT, wild-type.

identical to those of WT (5 weeks of treatment illustrated in Figure 8B). The two treatment durations had similar efficacy and did not alter vascular reactivity to ACh in WT animals. To test whether long-term B_1R blockade would influence the B_2R-driven vasomotricity, cerebrovascular responses to BK were tested. BK elicited a biphasic response (contraction followed by relaxation) in all groups, with a tendency, although not significant, to constrict more and dilate less in APP mice (Figure 8C). SSR240612 had no effect on vascular responses to BK, despite a

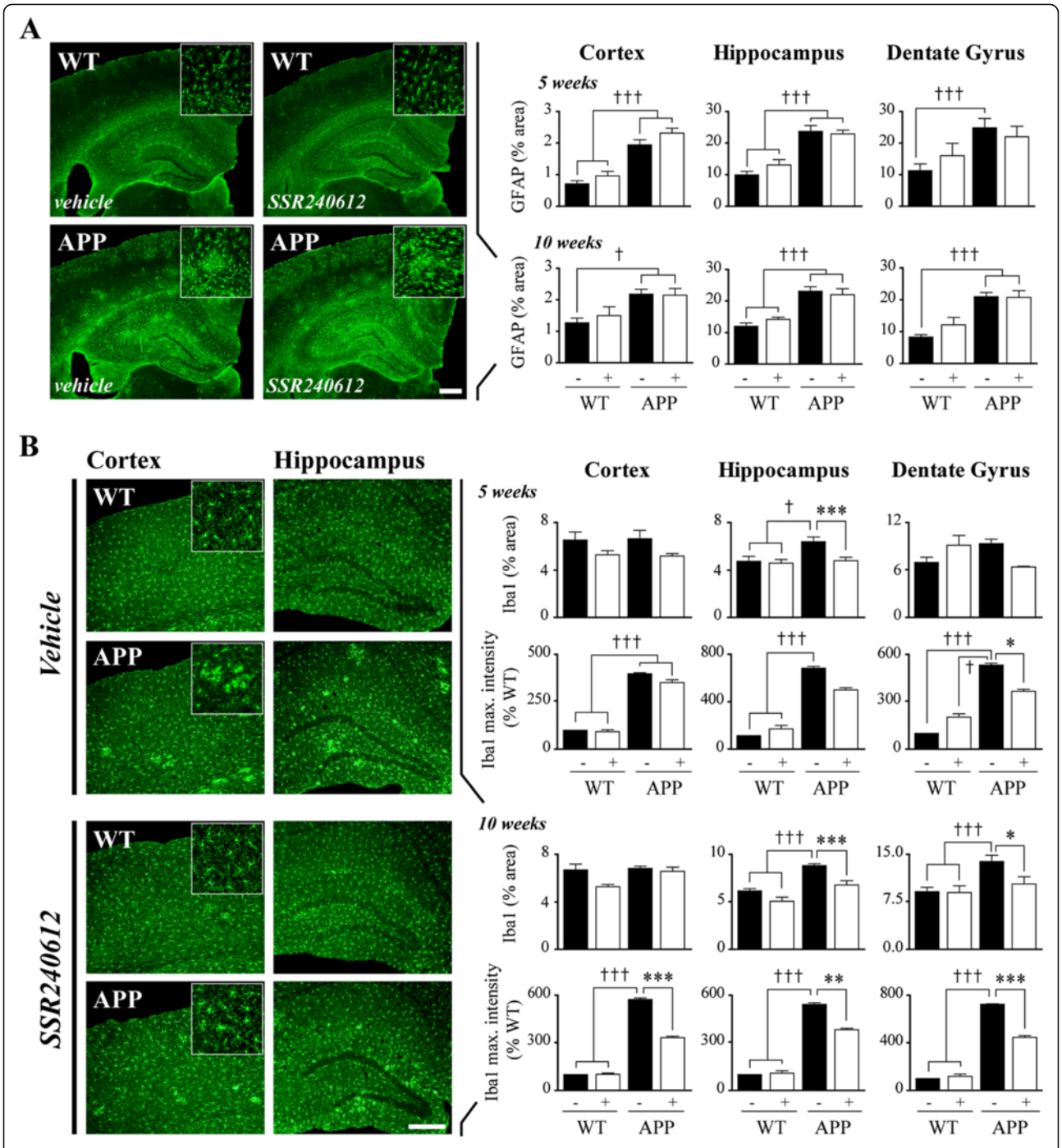

Figure 7 SSR240612 reduced microglial, but not astroglial, activation in the APP mouse brain. (A) As observed with glial fibrillary acidic protein (GFAP) immunolabeling (left), 5 and 10 weeks of treatment did not reduce astrocytosis in APP mice. **(B)** Following immunolabeling of microglial marker Iba1, SSR240612 treatments (10 weeks, left, compared to vehicle-treated mice) significantly reduced microglial activation (percentage of positive area) and aggregation (maximal labeling intensity). High magnifications are shown in insets in A and B. After 5 weeks of treatment, the effects were barely significant in hippocampus including the dentate gyrus (DG). Scale bars: 300 μm. Error bars represent SEM. *, †P <0.05; **, ††P <0.01; ***, †††P <0.001 (†: vs. WT; *: non-treated APP vs. treated APP). Two-way ANOVA followed by Newman-Keuls post hoc test. N = 5 to 6/group. APP, amyloid precursor protein; Iba1, ionized calcium-binding adaptor molecule 1; WT, wild-type.

Table 1 Counts of Iba1-positive cell bodies in the cortex and hippocampus from the two treatment cohorts

SSR 5 weeks	WT (n = 5)	WT-SSR (n = 5)	APP (n = 5)	APP-SSR (n = 4)
Cortex	542.5 ± 19.3	546.1 ± 46.5	536.3 ± 29.5	497.2 ± 8.8
Hippocampus	532.4 ± 36.8	553.9 ± 57.3	524.2 ± 37.1	518.2 ± 16.4
Dentate gyrus	418.1 ± 50.6	464.5 ± 62.9	439.6 ± 29.1	433.0 ± 60.8
SSR 10 weeks	**WT (n = 5)**	**WT-SSR (n = 5)**	**APP (n = 5)**	**APP-SSR (n = 5)**
Cortex	529.9 ± 27.1	557.8 ± 18.1	549.5 ± 11.9	576.4 ± 50.9
Hippocampus	608.2 ± 15.4	624.8 ± 33.2	669.8 ± 35.9	679.3 ± 62.2
Dentate gyrus	419.0 ± 22.7	423.9 ± 22.6	468.9 ± 15.2	466.0 ± 44.4

Data are means ± SEM from the number (n) of mice indicated in parentheses. *Iba1* ionized calcium-binding adaptor molecule 1, *SSR* SSR240612, *WT* wild-type, *APP* amyloid precursor protein.

slightly larger, not significant, dilation in treated WT mice at the highest agonist concentration (Figure 8C, Table 2). Although beyond the scope of the present investigation, further experiments could involve testing the effects of selective B_2R antagonists on the biphasic response to BK.

SSR240612 effects on brain and vascular BK receptors

The effects of SSR240612 on brain and vascular BK receptors were measured using western blot. B_1R protein levels were significantly increased only in the hippocampus from APP mice, as shown in the two mouse cohorts treated for 5 or 10 weeks (+41%, P <0.01; and +32%, P <0.05; respectively) (Figure 9A,B). SSR240612 treatment slightly reduced this upregulation in hippocampus, bringing B_1R protein levels in treated APP mice indistinguishable from those of WT controls after 10 weeks of drug delivery (Figure 9B, right). Neither genotype nor treatment altered B_2R protein levels in cortex and hippocampus. Knowing that B_2R and endothelial NOS (eNOS) activation mediate the effects of BK on brain arteries [33], their protein levels were measured in pial vessels. B_1R protein was not detected in vascular extracts (Figure 9C), confirming our immunohistochemical observations. However, in APP mice, B_2R and eNOS protein levels were increased in cerebral arteries (+40 to 50%; P <0.05), and both were normalized by SSR240612 administration independent of treatment duration (Figure 9C).

Discussion

Our study i) shows a selective astrocytic upregulation of B_1R, being almost exclusively associated with Aβ plaques, in the hippocampus of APP mice with impaired memory, and ii) demonstrates that chronic blockade of B_1R significantly improves learning and memory performances, cerebrovascular function, as well as several anatomopathological AD hallmarks in APP mice with a fully developed pathology. These findings strongly support a deleterious effect of kinin B_1R in AD pathogenesis.

Selective B_1R upregulation on Aβ plaque-associated astrocytes in hippocampus of APP mice

Previous *in vivo* studies in rats [17] or mice [18] showed increases in brain B_1R binding sites or protein levels after a single i.c.v. infusion of human $A\beta_{1\text{-}40}$. Here, with western blot analysis we found an upregulation of B_1R protein levels in the hippocampus, but not cerebral

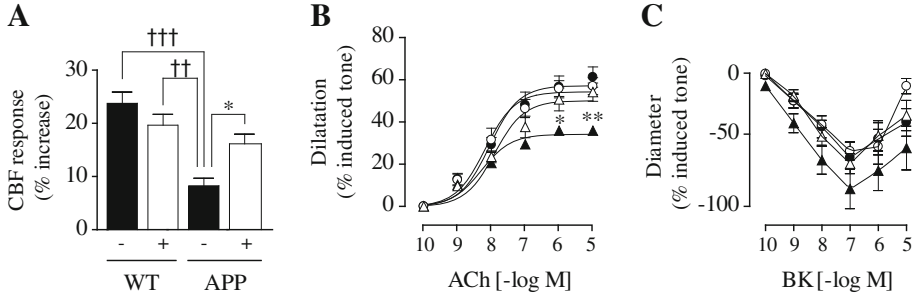

Figure 8 SSR240612 improved evoked CBF responses to sensory stimulation *in vivo* and cerebrovascular reactivity *ex vivo*. (A) In APP mice, B_1R antagonism (+) significantly ameliorated, but did not fully restore, the cerebral blood flow (CBF) response evoked by whisker stimulation. **(B,C)** Isolated and pressurized middle cerebral artery segments from APP mice (▲) displayed impaired dilation to acetylcholine (ACh) **(B)** and reduced, albeit non-significantly, the biphasic response (contraction followed by relaxation) to bradykinin (BK) **(C)**. Treatment with SSR240612 in APP mice (Δ) completely rescued dilation to ACh (B) but had no significant effect on vascular responses to BK **(C)**. Error bars represent SEM. **P* <0.05; ***P* <0.01, ****P* <0.001, Two-way ANOVA followed by Newman-Keuls post hoc test. N = 4 to 6/group. (● WT; ○ WT treated). APP, amyloid precursor protein; B_1R, bradykinin receptor 1; WT, wild-type.

Table 2 Effects of SSR240612 treatments on cerebrovascular responses to ACh and BK

SSR 5 weeks	WT (n = 4)	WT-SSR (n = 4)	APP (n = 4)	APP-SSR (n = 4)
ACh (EA_{max})	57.2 ± 3.0	54.3 ± 2.5	34.2 ± 2.0 ††	50.1 ± 3.3**
ACh (pD_2)	8.06 ± 0.2	8.19 ± 0.1	8.30 ± 0.2	7.91 ± 0.2
BK (max constr.)	−69.53 ± 13.2	−64.15 ± 7.3	−95.55 ± 16.4	−74.50 ± 8.3
BK (max dilat.)	−40.3 ± 11.4	−10.3 ± 6.4	−61.6 ± 18.1	−34.6 ± 12.6
SSR 10 weeks	**WT (n = 4)**	**WT-SSR (n = 5)**	**APP (n = 5)**	**APP-SSR (n = 5)**
ACh (EA_{max})	51.2 ± 2.7	67.8 ± 3.3	32.5 ± 1.9 †	49.2 ± 3.2 *
ACh (pD_2)	8.03 ± 0.1	7.79 ± 0.1	8.37 ± 0.18	8.17 ± 0.2
BK (max constr.)	−54.11 ± 6.4	−77.67 ± 7.8	−70.77 ± 7.5	−63.78 ± 9.2
BK (max dilat.)	−23.5 ± 5.5	−8.6 ± 9.2	−44.9 ± 8.3	−31.3 ± 9.8

Data are means ± SEM from the number (n) of mice indicated in parentheses and expressed as the agonist maximal response (EA_{max}) or affinity (pD2, -log[EC50]). EA_{max} (%) is the maximal dilation to ACh. For agonist response to BK, both the maximal constriction and dilatation from the induced tone (%) are indicated. Values for BK are negative, the zero value being the induced tone. $^{\dagger}P$ <0.05, $^{\dagger\dagger}P$ <0.01 when compared to non-treated WT controls; $^{*}P$ <0.05, $^{**}P$ <0.01 when compared to non-treated APP mice. *SSR* SSR240612, *ACh* acetylcholine, *BK* bradykinin, *WT* wild-type, *APP* amyloid precursor protein.

cortex of approximately 11- to 12-month-old APP mice. Furthermore, using the cellular resolution of immunocytochemistry, we confirmed that B_1R were upregulated in the hippocampus of APP mice, particularly in the hilus of the DG, a key segment of the entorhinal-hippocampal network for learning and memory that is impaired early by APP/Aβ overproduction [47]. Interestingly, recent evidence suggests that upregulation of B_1R might occur in early stages of AD-associated neuroinflammation [2], particularly in the hippocampus where components of the KKS are activated in response to inflammatory stimuli [48].

Astrocytes and microglia are instrumental in the neuroinflammatory processes associated with AD pathogenesis [49], and activation of astrocytes and microglia can be evidenced in the brain of APP mice with their respective typical association outside and within Aβ plaques [50]. Yet, the prominent finding from double-immunofluorescence experiments was that upregulation of B_1R was limited to astrocytes, mainly those located in the vicinity of Aβ deposits, that displayed characteristics of reactive astrocytes such as hypertrophic processes and soma, and upregulated GFAP immunostaining [51]. Our findings add to the previously reported upregulation of B_1R on glial or neuronal cells in various pathologies, including in the brain of epileptic patients [52] and spinal cord of diabetic rats [53].

In contrast to a recent report of B_1R upregulation in brain microvessels of Tg-SwDI mice, published online while our work was under review [54], we did not detect cerebrovascular B_1R expression in our 12-month-old APP mice. Beyond the use of different anti-B_1R primary antibodies, this apparent discrepancy is likely due to the robust deposition of cerebrovascular amyloid (CAA) in Tg-SwDI mice [55]. Indeed, J20 APP mice at the age used in our study are literally free of CAA [30]. Together, these findings reinforce our conclusion that astroglial B_1R upregulation is associated primarily, if not exclusively, with aggregated Aβ species.

SSR240612 and recovery of cognitive deficits in APP mice

We found that chronic B_1R antagonism improved spatial learning and memory in APP mice, abilities that depend largely on hippocampal integrity [56]. Moreover, prolonged B_1R blockade enhanced the baseline levels of the memory-related Egr-1 protein in the DG, a brain region previously associated in APP mice with cognitive deficits, reduced immediate-early gene expression and altered synaptic activity [57,58]. Although further experiments would be required to confirm this hypothesis, it is conceivable that under chronic B_1R blockade with SSR240612 in APP mice, BK can then act on its normal target and preferentially activate constitutive B_2R that are considered neuroprotective and able to prevent memory loss [59].

The findings of decreased soluble $A\beta_{1\text{-}42}$ and Aβ plaque load in both cortex and hippocampus after SSR240612 treatment suggested that B_1R blockade interfered with the amyloidogenic cascade and, particularly, with the deposition of the fast aggregating $A\beta_{1\text{-}42}$ species. Interestingly, long-term B_1R blockade in APP mice resulted in increased production of MMP9 that is known to promote non-amyloidogenic processing of APP [60], and in increased cerebrovascular LRP-1 immunoreactivity, a vascular mediator of Aβ efflux from brain to blood [61]. Our results may thus suggest a stimulated Aβ clearance at the BBB following B_1R blockade. To date, both soluble [62,63] and insoluble Aβ levels have been incriminated in cerebrovascular and cognitive deficits observed in APP mice [64,65], but there is also strong evidence for no relationship between the Aβ pathology and cognitive performance in APP mice [30,66,67]. We cannot ascertain whether or not the normalized memory performance in APP mice after

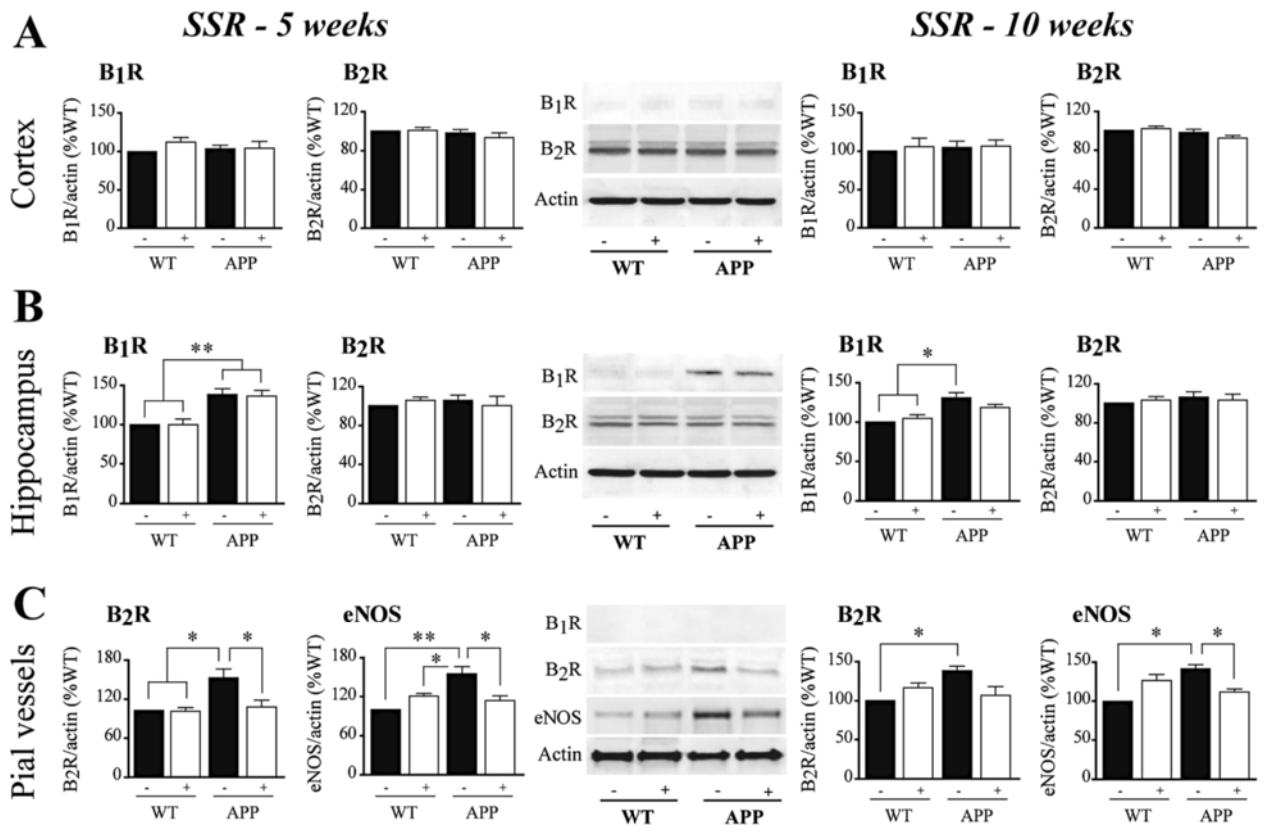

Figure 9 Effects of SSR240612 treatment on cerebral kinin receptors and on endothelial NOS and vascular B_2R protein levels. **(A,B)** Single bands were detected at 37 and 135 kDa by anti-B_1R and anti-eNOS antibodies, respectively, whereas anti-B_2R antibodies decorated a characteristic doublet around 42 kDa. No change in cortical B_1R and B_2R **(A)** or in hippocampal B_2R **(B)** protein levels was observed, but B_1R were upregulated in the hippocampus of APP mice **(B)**, with no effect of treatment. **(C)** In pial vessels, protein levels of endothelial NOS (eNOS) and B_2R were normalized by B_1R blockade. Blots images illustrate the 5 weeks of treatment. *P <0.05; **P <0.01, Two-way ANOVA followed by Newman-Keuls post hoc test. Blots images illustrate the 5 weeks of treatment. N = 5 to 6/group. APP, amyloid precursor protein; B_2R, bradykinin receptor 2.

B_1R blockade is related to the concurrent decreases in soluble $A\beta_{1\text{-}42}$ species and Aβ plaque load. However, the relationships between high Aβ plaque load and low cognitive scores - particularly striking in the DG - and of high Aβ plaque load and low LRP-1 immunostaining (Figure 10) were shifted toward low plaque load and high cognitive performance, and toward low plaque load and high LRP-1 following SSR240612 treatment, suggesting a negative impact of Aβ on cognition possibly due to its lack of clearance from brain.

SSR240612 effects on reactive astrocytes and microglia

Aβ is the main initiating factor of the inflammatory cascade in APP mice, and specific Aβ domains can stimulate the KKS [68], and it has been argued that brain injury in AD is primarily caused by Aβ-induced neuroinflammation [69]. Interesting to the present study was that B_1R antagonism selectively reduced microglial activation, and most strikingly reactive microglia associated with Aβ plaques. Suggestive of microglial migration and aggregation around plaques, we show that despite an unchanged total microglial cells number in APP mice brain, the intensity of anti-microglia staining is increased in APP compared to WT controls, and significantly reduced following B_1R blockade. It thus seems that the reduction in Aβ plaque load contributed to the silencing of the reactive microglial cells. This would be consistent with Aβ-induced migration of phagocytic microglia, and with plaque-associated reactive microglia contributing to the inflammatory response and exhibiting a neurotoxic phenotype [70,71]. Intense and patchy GFAP-immunostained astrocytes persisted after SSR240612 treatment, suggesting that astrocytes have maintained a reactive phenotype, as supported by the enduring increases in B_1R protein levels in activated astrocytes in APP mouse hippocampus (Figure 2). This might indicate a compensatory astroglial activation in response to the reduction in microgliosis [72], possibly related to the ability of reactive astrocytes to attenuate microglia-derived neurotoxicity [44].

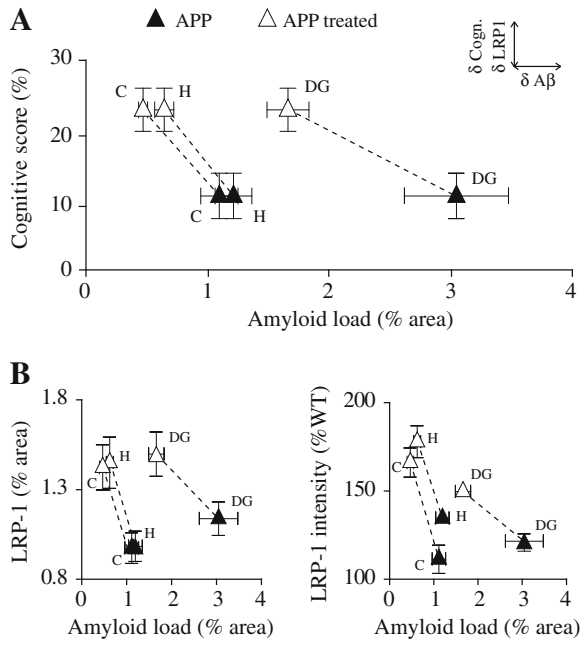

Figure 10 Relationships between cognitive performances, amyloidosis and LRP-1 expression in APP mouse brain. **(A)** Relationship between Aβ plaque load and cognitive score (see Material and Methods). **(B)** Relationship between Aβ plaque load and LRP-1 immunoreactivity (left, % area; right, intensity). Illustration for the 10-week treatment, but similar relationships were obtained after the 5-week treatment. Error bars represent SEM. N = 5/group (▲ APP; Δ APP treated). Aβ, amyloid-beta; APP, amyloid precursor protein; C, cortex; H, hippocampus; DG, dentate gyrus; LRP-1, lipoprotein receptor-related protein.

Improvement of cerebrovascular function following B_1R blockade

A remarkable outcome from the present study was the normalization of CBF responses and cerebrovascular reactivity in adult APP mice by chronic B_1R antagonism, irrespective of the treatment duration. Growing evidence supports cerebrovascular impairment as an early event of AD pathogenesis [1]. Since B_1R blockade failed to reduce soluble $A\beta_{1-40}$ in APP mice, commonly perceived as a seed for $A\beta_{1-42}$ deposition in brain vessels leading to CAA [73], recovery of cerebrovascular reactivity in APP mice likely happened through reduction of soluble $A\beta_{1-42}$ since they display virtually no CAA at this age [30]. $A\beta_{1-42}$ is detrimental to cerebrovascular function [45] through increased oxidative stress [31,74] and inflammation [75,76]. Hence, cerebrovascular recovery likely resulted, at least in part, from the ability of SSR240612 to antagonize the B_1R-mediated production of vascular NADPH oxidase-derived reactive oxygen species [10] and inflammatory cytokines [77], as recently documented in aorta from a rat model of insulin resistance. In treated APP mice, SSR240612 normalized the increased levels of B_2R and eNOS, two key proteins in endothelial-mediated vasomotor responses, which are known to be upregulated by oxidative stress and inflammation [8]. Hence, the high eNOS protein levels in APP mice may reflect a compensatory upregulation in response to the reduced NO bioavailability following its trapping by reactive oxygen species [31,74], as also reported in a model of diabetes-associated vascular disease [78].

Conclusions

Our findings indicate that upregulation of B_1R in APP mice results in deleterious effects on the cerebral vasculature and brain parenchyma. They further demonstrate the capacity of the B_1R antagonist SSR240612 to abrogate amyloidosis, cerebrovascular and memory deficits. These observations provide support for a neuroprotective role for B_1R antagonism in AD, pointing to the need to better understand the role of the KKS in AD pathogenesis.

Abbreviations

5-HT: 5-hydroxytryptamine (serotonin); Aβ: Amyloid-beta; ACh: Acetylcholine; AD: Alzheimer's disease; APP: Amyloid precursor protein; B_1R: Bradykinin receptor 1; BACE: Beta-site APP-cleaving enzyme (β-secretase); BBB: Blood–brain barrier; BK: Bradykinin; CAA: Cerebrovascular amyloid; CBF: Cerebral blood flow; CD11b: Cluster of differentiation molecule 11b; CSF: Cerebrospinal fluid; DG: Dentate gyrus; DMSO: Dimethyl sulfoxide; EAmax: Maximal response; Egr-1: Early growth response protein 1; ELISA: Enzyme-linked immunosorbent assay; eNOS: Endothelial nitric oxide synthase; GFAP: Glial fibrillary acidic protein; Iba1: Ionized calcium-binding adaptor molecule 1; i.c.v.: Intracerebroventricular; IHC: Immunohisto chemistry; KKS: Kallikrein-kinin system; KO: Knockout; LRP-1: Lipoprotein receptor-related protein 1; MCA: Middle cerebral artery; MMP9: Matrix metallopeptidase 9; PDGF: Platelet-derived growth factor; PFA: Paraformaldehyde; RT: Room temperature; SEM: Standard error of the mean; WB: Western blot; WT: Wild-type.

Competing interests

The authors declare that they have no competing interests.

Authors' contributions

BL designed the study and performed all experiments and statistical analyses - except for CBF measurements of the 5-week treatment cohort - and drafted the manuscript (text and figures). XKT performed the CBF measurements for the 5-week treatment cohort and provided technical advises at all steps of the study. KL developed and characterized the primary anti-B_1R and -B_2R antibodies under RC's supervision. RC co-supervised BL's work, participated in the design of the study and helped draft the manuscript. EH designed and supervised all steps of the study, and corrected the manuscript. All authors read and approved the final manuscript.

Acknowledgments

Supported by research grants from Canadian Institutes of Health Research (CIHR, MOP-84275 to EH and MOP-79471 to RC). BL held a postdoctoral fellowship award from the Alzheimer Society of Canada. The authors thank Dr. L. Mucke (Gladstone Institute of Neurological Disease and Department of Neurology, UCSF, CA, USA), the J. David Gladstone Institutes for the $hAPP_{Swe,Ind}$ transgenic mouse breeders, and Sanofi-Aventis Laboratories for their generous supply of SSR240612. The authors also thank Drs. Yiu Chung Tse, Tak Pan Wong, Nektaria Nicolakakis, Brice Ongali and Tahar Aboulkassim for scientific advice and technical assistance.

Author details

[1]Laboratory of Cerebrovascular Research, Montreal Neurological Institute, McGill University, 3801 University Street, Montréal, QC H3A 2B4, Canada. [2]Department of Physiology, Faculty of Medicine, Université de Montréal, 2900 Boulevard Edouard-Montpetit, Montréal, QC H3T 1J4, Canada.

Received: 3 March 2013 Accepted: 20 April 2013
Published: 4 May 2013

References

1. Nicolakakis N, Hamel E: **Neurovascular function in Alzheimer's disease patients and experimental models.** *J Cereb Blood Flow Metab* 2011, **31:**1354–1370.
2. Viel TA, Buck HS: **Kallikrein-kinin system mediated inflammation in Alzheimer's disease in vivo.** *Curr Alzheimer Res* 2011, **8:**59–66.
3. Couture R, Lindsey CJ, Quirion R, Bjorklund A, Hokfelt T: **Brain kallikrein-kinin system: from receptors to neuronal pathways and physiological functions.** In *Handbook of Chemical Neuroanatomy. Volume 16.* Oxford: Elsevier Science; 2000:241–300.
4. Marceau F, Sabourin T, Houle S, Fortin JP, Petitclerc E, Molinaro G, Adam A: **Kinin receptors: functional aspects.** *Int Immunopharmacol* 2002, **2:**1729–1739.
5. Hamel E, Edvinsson L, MacKenzie ET: **Heterogeneous vasomotor responses of anatomically distinct feline cerebral arteries.** *Br J Pharmacol* 1988, **94:**423–436.
6. Wahl M, Whalley ET, Unterberg A, Schilling L, Parsons AA, Baethmann A, Young AR: **Vasomotor and permeability effects of bradykinin in the cerebral microcirculation.** *Immunopharmacology* 1996, **33:**257–263.
7. De Brito GH, Carayon P, Ferrari B, Couture R: **Contribution of the central dopaminergic system in the anti-hypertensive effect of kinin B1 receptor antagonists in two rat models of hypertension.** *Neuropeptides* 2010, **44:**191–198.
8. Groger M, Lebesgue D, Pruneau D, Relton J, Kim SW, Nussberger J, Plesnila N: **Release of bradykinin and expression of kinin B2 receptors in the brain: role for cell death and brain edema formation after focal cerebral ischemia in mice.** *J Cereb Blood Flow Metab* 2005, **25:**978–989.
9. Ongali B, Hellal F, Rodi D, Plotkine M, Marchand-Verrecchia C, Pruneau D, Couture R: **Autoradiographic analysis of mouse brain kinin B1 and B2 receptors after closed head trauma and ability of Anatibant mesylate to cross the blood–brain barrier.** *J Neurotrauma* 2006, **23:**696–707.
10. Dias JP, Talbot S, Senecal J, Carayon P, Couture R: **Kinin B1 receptor enhances the oxidative stress in a rat model of insulin resistance: outcome in hypertension, allodynia and metabolic complications.** *PLoS One* 2010, **5:**e12622.
11. Gorelick PB: **Risk factors for vascular dementia and Alzheimer disease.** *Stroke* 2004, **35:**2620–2622.
12. Lacoste B, Tong XK, Lahjouji K, Couture R, Hamel E: **Bradykinin B1 receptor blockade in the treatment of Alzheimer's disease: improvement of cognitive and cerebrovascular functions, and reduction of amyloidosis [abstract].** *Alzheimer's & Dementia* 2011, **7:**S512–S513.
13. Lacoste B, Lahjouji K, Tong XK, Couture R, Hamel E: **Improvement of cognitive and cerebrovascular functions by bradykinin B1 receptor antagonism in the APP mouse model of Alzheimer's disease [abstract].** In *Proceedings of the Society for Neuroscience Annual Meeting: November 16, 2010.* San Diego, CA [Neuroscience Meeting Planner 2010 online, Program No.556.26/M3.].
14. Bergamaschini L, Parnetti L, Pareyson D, Canziani S, Cugno M, Agostoni A: **Activation of the contact system in cerebrospinal fluid of patients with Alzheimer disease.** *Alzheimer Dis Assoc Disord* 1998, **12:**102–108.
15. Wang Q, Wang J: **Injection of bradykinin or cyclosporine A to hippocampus induces Alzheimer-like phosphorylation of Tau and abnormal behavior in rats.** *Chin Med J (Engl)* 2002, **115:**884–887.
16. Iores-Marcal LM, Viel TA, Buck HS, Nunes VA, Gozzo AJ, Cruz-Silva I, Miranda A, Shimamoto K, Ura N, Araujo MS: **Bradykinin release and inactivation in brain of rats submitted to an experimental model of Alzheimer's disease.** *Peptides* 2006, **27:**3363–3369.
17. Viel TA, Lima Caetano A, Nasello AG, Lancelotti CL, Nunes VA, Araujo MS, Buck HS: **Increases of kinin B1 and B2 receptors binding sites after brain infusion of amyloid-beta 1–40 peptide in rats.** *Neurobiol Aging* 2008, **29:**1805–1814.
18. Prediger RD, Medeiros R, Pandolfo P, Duarte FS, Passos GF, Pesquero JB, Campos MM, Calixto JB, Takahashi RN: **Genetic deletion or antagonism of kinin B(1) and B(2) receptors improves cognitive deficits in a mouse model of Alzheimer's disease.** *Neuroscience* 2008, **151:**631–643.
19. Raslan F, Schwarz T, Meuth SG, Austinat M, Bader M, Renne T, Roosen K, Stoll G, Siren AL, Kleinschnitz C: **Inhibition of bradykinin receptor B1 protects mice from focal brain injury by reducing blood–brain barrier leakage and inflammation.** *J Cereb Blood Flow Metab* 2010, **30:**1477–1486.
20. Zipser BD, Johanson CE, Gonzalez L, Berzin TM, Tavares R, Hulette CM, Vitek MP, Hovanesian V, Stopa EG: **Microvascular injury and blood–brain barrier leakage in Alzheimer's disease.** *Neurobiol Aging* 2007, **28:**977–986.
21. Gotz J, Ittner LM: **Animal models of Alzheimer's disease and frontotemporal dementia.** *Nat Rev Neurosci* 2008, **9:**532–544.
22. Mucke L, Masliah E, Yu GQ, Mallory M, Rockenstein EM, Tatsuno G, Hu K, Kholodenko D, Johnson-Wood K, McConlogue L: **High-level neuronal expression of abeta 1–42 in wild-type human amyloid protein precursor transgenic mice: synaptotoxicity without plaque formation.** *J Neurosci* 2000, **20:**4050–4058.
23. Gougat J, Ferrari B, Sarran L, Planchenault C, Poncelet M, Maruani J, Alonso R, Cudennec A, Croci T, Guagnini F, Urban-Szabo K, Martinolle JP, Soubrié P, Finance O, Le Fur G: **SSR240612 [(2R)-2-[((3R)-3-(1,3-benzodioxol-5-yl)-3-[[(6-methoxy-2-naphthyl)sulfonyl]amino]propanoyl)amino]-3-(4-[[2R,6S)-2,6-dimethylpiperidinyl]methyl]pheny l)-N-isopropyl-N-methylpropanamide hydrochloride], a new nonpeptide antagonist of the bradykinin B1 receptor: biochemical and pharmacological characterization.** *J Pharmacol Exp Ther* 2004, **309:**661–669.
24. Fincham CI, Bressan A, Paris M, Rossi C, Fattori D: **Bradykinin receptor antagonists-a review of the patent literature 2005–2008.** *Expert Opin Ther Pat* 2009, **19:**919–941.
25. Pouliot M, Hetu S, Lahjouji K, Couture R, Vaucher E: **Modulation of retinal blood flow by kinin B receptor in Streptozotocin-diabetic rats.** *Exp Eye Res* 2011, **92:**482–489.
26. Bulut OP, Dipp S, El-Dahr S: **Ontogeny of bradykinin B1 receptors in the mouse kidney.** *Pediatr Res* 2009, **66:**519–523.
27. Hsia AY, Masliah E, McConlogue L, Yu GQ, Tatsuno G, Hu K, Kholodenko D, Malenka RC, Nicoll RA, Mucke L: **Plaque-independent disruption of neural circuits in Alzheimer's disease mouse models.** *Proc Natl Acad Sci U S A* 1999, **96:**3228–3233.
28. Nicolakakis N, Aboulkassim T, Ongali B, Lecrux C, Fernandes P, Rosa-Neto P, Tong XK, Hamel E: **Complete rescue of cerebrovascular function in aged Alzheimer's disease transgenic mice by antioxidants and pioglitazone, a peroxisome proliferator-activated receptor gamma agonist.** *J Neurosci* 2008, **28:**9287–9296.
29. Deipolyi AR, Fang S, Palop JJ, Yu GQ, Wang X, Mucke L: **Altered navigational strategy use and visuospatial deficits in hAPP transgenic mice.** *Neurobiol Aging* 2008, **29:**253–266.
30. Tong XK, Lecrux C, Hamel E: **Age-dependent rescue by Simvastatin of Alzheimer's disease cerebrovascular and memory deficits.** *J Neurosci* 2012, **32:**4705–4715.
31. Tong XK, Nicolakakis N, Kocharyan A, Hamel E: **Vascular remodeling versus amyloid beta-induced oxidative stress in the cerebrovascular dysfunctions associated with Alzheimer's disease.** *J Neurosci* 2005, **25:**11165–11174.
32. Satvat E, Schmidt B, Argraves M, Marrone DF, Markus EJ: **Changes in task demands alter the pattern of zif268 expression in the dentate gyrus.** *J Neurosci* 2011, **31:**7163–7167.
33. Gorlach C, Wahl M: **Bradykinin dilates rat middle cerebral artery and its large branches via endothelial B2 receptors and release of nitric oxide.** *Peptides* 1996, **17:**1373–1378.
34. Worley PF, Christy BA, Nakabeppu Y, Bhat RV, Cole AJ, Baraban JM: **Constitutive expression of zif268 in neocortex is regulated by synaptic activity.** *Proc Natl Acad Sci U S A* 1991, **88:**5106–5110.
35. Jones MW, Errington ML, French PJ, Fine A, Bliss TV, Garel S, Charnay P, Bozon B, Laroche S, Davis S: **A requirement for the immediate early gene Zif268 in the expression of late LTP and long-term memories.** *Nat Neurosci* 2001, **4:**289–296.
36. Dickey CA, Loring JF, Montgomery J, Gordon MN, Eastman PS, Morgan D: **Selectively reduced expression of synaptic plasticity-related genes in amyloid precursor protein + presenilin-1 transgenic mice.** *J Neurosci* 2003, **23:**5219–5226.
37. Deane R, Wu Z, Sagare A, Davis J, Du Yan S, Hamm K, Xu F, Parisi M, LaRue B, Hu HW, Spijkers P, Guo H, Song X, Lenting PJ, Van Nostrand WE, Zlokovic BV: **LRP/amyloid beta-peptide interaction mediates differential brain efflux of Abeta isoforms.** *Neuron* 2004, **43:**333–344.
38. Bell RD, Zlokovic BV: **Neurovascular mechanisms and blood–brain barrier disorder in Alzheimer's disease.** *Acta Neuropathol* 2009, **118:**103–113.
39. Xu G, Green C, Fromholt S, Borchelt D: **Reduction of low-density lipoprotein receptor-related protein (LRP1) in hippocampal neurons does not proportionately reduce, or otherwise alter, amyloid deposition in APPswe/PS1dE9 transgenic mice.** *Alzheimer's Research & Therapy* 2012, **4:**12.
40. Liu LY, Zheng H, Xiao HL, She ZJ, Zhao SM, Chen ZL, Zhou GM: **Comparison of blood-nerve barrier disruption and matrix metalloprotease-9 expression in injured central and peripheral nerves in mice.** *Neurosci Lett* 2008, **434:**155–159.

41. Wang Z, Meng CJ, Shen XM, Shu Z, Ma C, Zhu GQ, Liu HX, He WC, Sun XB, Huo L, Zhang J, Chen G: **Potential contribution of hypoxia-inducible factor-1alpha, aquaporin-4, and matrix metalloproteinase-9 to blood–brain barrier disruption and brain edema after experimental subarachnoid hemorrhage.** *J Mol Neurosci* 2012, **48:**273–280.
42. Yan P, Hu X, Song H, Yin K, Bateman RJ, Cirrito JR, Xiao Q, Hsu FF, Turk JW, Xu J, Hsu CY, Holtzman DM, Lee JM: **Matrix metalloproteinase-9 degrades amyloid-beta fibrils in vitro and compact plaques in situ.** *J Biol Chem* 2006, **281:**24566–24574.
43. Yin KJ, Cirrito JR, Yan P, Hu X, Xiao Q, Pan X, Bateman R, Song H, Hsu FF, Turk J, Xu J, Hsu CY, Mills JC, Holtzman DM, Lee JM: **Matrix metalloproteinases expressed by astrocytes mediate extracellular amyloid-beta peptide catabolism.** *J Neurosci* 2006, **26:**10939–10948.
44. von Bernhardi R, Ramirez G: **Microglia-astrocyte interaction in Alzheimer's disease: friends or foes for the nervous system?** *Biol Res* 2001, **34:**123–128.
45. Niwa K, Kazama K, Younkin SG, Carlson GA, Iadecola C: **Alterations in cerebral blood flow and glucose utilization in mice overexpressing the amyloid precursor protein.** *Neurobiol Dis* 2002, **9:**61–68.
46. Niwa K, Kazama K, Younkin L, Younkin SG, Carlson GA, Iadecola C: **Cerebrovascular autoregulation is profoundly impaired in mice overexpressing amyloid precursor protein.** *Am J Physiol Heart Circ Physiol* 2002, **283:**H315–H323.
47. Harris JA, Devidze N, Verret L, Ho K, Halabisky B, Thwin MT, Kim D, Hamto P, Lo I, Yu GQ, Palop JJ, Masliah E, Mucke L: **Transsynaptic progression of amyloid-beta-induced neuronal dysfunction within the entorhinal-hippocampal network.** *Neuron* 2010, **68:**428–441.
48. Chen EY, Emerich DF, Bartus RT, Kordower JH: **B2 bradykinin receptor immunoreactivity in rat brain.** *J Comp Neurol* 2000, **427:**1–18.
49. Tuppo EE, Arias HR: **The role of inflammation in Alzheimer's disease.** *Int J Biochem Cell Biol* 2005, **37:**289–305.
50. Itagaki S, McGeer PL, Akiyama H, Zhu S, Selkoe D: **Relationship of microglia and astrocytes to amyloid deposits of Alzheimer disease.** *J Neuroimmunol* 1989, **24:**173–182.
51. Pekny M, Nilsson M: **Astrocyte activation and reactive gliosis.** *Glia* 2005, **50:**427–434.
52. Perosa SR, Arganaraz GA, Goto EM, Costa LG, Konno AC, Varella PP, Santiago JF, Pesquero JB, Canzian M, Amado D, Yacubian EM, Carrete H Jr, Centeno RS, Cavalheiro EA, Silva JA Jr, Mazzacoratti Mda G: **Kinin B1 and B2 receptors are overexpressed in the hippocampus of humans with temporal lobe epilepsy.** *Hippocampus* 2007, **17:**26–33.
53. Talbot S, Theberge-Turmel P, Liazoghli D, Senecal J, Gaudreau P, Couture R: **Cellular localization of kinin B1 receptor in the spinal cord of streptozotocin-diabetic rats with a fluorescent [Nalpha-Bodipy]-des-Arg9-bradykinin.** *J Neuroinflammation* 2009, **6:**11.
54. Passos GF, Medeiros R, Cheng D, Vasilevko V, Laferla FM, Cribbs DH: **The bradykinin B receptor regulates abeta deposition and neuroinflammation in Tg-SwDI mice.** *Am J Pathol* 2013, **182:**1740–1749.
55. Davis J, Xu F, Miao J, Previti ML, Romanov G, Ziegler K, Van Nostrand WE: **Deficient cerebral clearance of vasculotropic mutant Dutch/Iowa Double A beta in human A betaPP transgenic mice.** *Neurobiol Aging* 2006, **27:**946–954.
56. Broadbent NJ, Squire LR, Clark RE: **Spatial memory, recognition memory, and the hippocampus.** *Proc Natl Acad Sci U S A* 2004, **101:**14515–14520.
57. Palop JJ, Chin J, Bien-Ly N, Massaro C, Yeung BZ, Yu GQ, Mucke L: **Vulnerability of dentate granule cells to disruption of arc expression in human amyloid precursor protein transgenic mice.** *J Neurosci* 2005, **25:**9686–9693.
58. Chapman PF, White GL, Jones MW, Cooper-Blacketer D, Marshall VJ, Irizarry M, Younkin L, Good MA, Bliss TV, Hyman BT, Younkin SG, Hsiao KK: **Impaired synaptic plasticity and learning in aged amyloid precursor protein transgenic mice.** *Nat Neurosci* 1999, **2:**271–276.
59. Noda M, Kariura Y, Pannasch U, Nishikawa K, Wang L, Seike T, Ifuku M, Kosai Y, Wang B, Nolte C, Aoki S, Kettenmann H, Wada K: **Neuroprotective role of bradykinin because of the attenuation of pro-inflammatory cytokine release from activated microglia.** *J Neurochem* 2007, **101:**397–410.
60. Fragkouli A, Papatheodoropoulos C, Georgopoulos S, Stamatakis A, Stylianopoulou F, Tsilibary EC, Tzinia AK: **Enhanced neuronal plasticity and elevated endogenous sAPPalpha levels in mice over-expressing MMP9.** *J Neurochem* 2012, **121:**239–251.
61. Zlokovic BV, Deane R, Sagare AP, Bell RD, Winkler EA: **Low-density lipoprotein receptor-related protein-1: a serial clearance homeostatic mechanism controlling Alzheimer's amyloid beta-peptide elimination from the brain.** *J Neurochem* 2010, **115:**1077–1089.
62. Cheng IH, Scearce-Levie K, Legleiter J, Palop JJ, Gerstein H, Bien-Ly N, Puolivali J, Lesne S, Ashe KH, Muchowski PJ, Mucke L: **Accelerating amyloid-beta fibrillization reduces oligomer levels and functional deficits in Alzheimer disease mouse models.** *J Biol Chem* 2007, **282:**23818–23828.
63. Walsh DM, Klyubin I, Fadeeva JV, Cullen WK, Anwyl R, Wolfe MS, Rowan MJ, Selkoe DJ: **Naturally secreted oligomers of amyloid beta protein potently inhibit hippocampal long-term potentiation in vivo.** *Nature* 2002, **416:**535–539.
64. Park JH, Widi GA, Gimbel DA, Harel NY, Lee DH, Strittmatter SM: **Subcutaneous Nogo receptor removes brain amyloid-beta and improves spatial memory in Alzheimer's transgenic mice.** *J Neurosci* 2006, **26:**13279–13286.
65. Han BH, Zhou ML, Abousaleh F, Brendza RP, Dietrich HH, Koenigsknecht-Talboo J, Cirrito JR, Milner E, Holtzman DM, Zipfel GJ: **Cerebrovascular dysfunction in amyloid precursor protein transgenic mice: contribution of soluble and insoluble amyloid-beta peptide, partial restoration via gamma-secretase inhibition.** *J Neurosci* 2008, **28:**13542–13550.
66. Park L, Zhou P, Pitstick R, Capone C, Anrather J, Norris EH, Younkin L, Younkin S, Carlson G, McEwen BS, Iadecola C: **Nox2-derived radicals contribute to neurovascular and behavioral dysfunction in mice overexpressing the amyloid precursor protein.** *Proc Natl Acad Sci U S A* 2008, **105:**1347–1352.
67. Li L, Cao D, Kim H, Lester R, Fukuchi K: **Simvastatin enhances learning and memory independent of amyloid load in mice.** *Ann Neurol* 2006, **60:**729–739.
68. Bergamaschini L, Donarini C, Foddi C, Gobbo G, Parnetti L, Agostoni A: **The region 1–11 of Alzheimer amyloid-beta is critical for activation of contact-kinin system.** *Neurobiol Aging* 2001, **22:**63–69.
69. McGeer PL, McGeer EG: **The inflammatory response system of brain: implications for therapy of Alzheimer and other neurodegenerative diseases.** *Brain Res Brain Res Rev* 1995, **21:**195–218.
70. Giulian D, Haverkamp LJ, Li J, Karshin WL, Yu J, Tom D, Li X, Kirkpatrick JB: **Senile plaques stimulate microglia to release a neurotoxin found in Alzheimer brain.** *Neurochem Int* 1995, **27:**119–137.
71. Wyss-Coray T: **Inflammation in Alzheimer disease: driving force, bystander or beneficial response?** *Nat Med* 2006, **12:**1005–1015.
72. Lu DC, Zador Z, Yao J, Fazlollahi F, Manley GT: **Aquaporin-4 reduces post-traumatic seizure susceptibility by promoting astrocytic glial scar formation in mice.** *J Neurotrauma* 2011. Epub ahead of print.
73. Rhodin JA, Thomas T: **A vascular connection to Alzheimer's disease.** *Microcirculation* 2001, **8:**207–220.
74. Park L, Anrather J, Zhou P, Frys K, Pitstick R, Younkin S, Carlson GA, Iadecola C: **NADPH-oxidase-derived reactive oxygen species mediate the cerebrovascular dysfunction induced by the amyloid beta peptide.** *J Neurosci* 2005, **25:**1769–1777.
75. Townsend KP, Obregon D, Quadros A, Patel N, Volmar C, Paris D, Mullan M: **Proinflammatory and vasoactive effects of Abeta in the cerebrovasculature.** *Ann N Y Acad Sci* 2002, **977:**65–76.
76. Yu D, Corbett B, Yan Y, Zhang GX, Reinhart P, Cho SJ, Chin J: **Early cerebrovascular inflammation in a transgenic mouse model of Alzheimer's disease.** *Neurobiol Aging* 2012, **33:**2942–2947.
77. Dias JP, Couture R: **Suppression of vascular inflammation by kinin B1 receptor antagonism in a rat model of insulin resistance.** *J Cardiovasc Pharmacol* 2012, **60:**61–69.
78. Ding H, Aljofan M, Triggle CR: **Oxidative stress and increased eNOS and NADPH oxidase expression in mouse microvessel endothelial cells.** *J Cell Physiol* 2007, **212:**682–689.

doi:10.1186/1742-2094-10-57
Cite this article as: Lacoste *et al.*: Cognitive and cerebrovascular improvements following kinin B_1 receptor blockade in Alzheimer's disease mice. *Journal of Neuroinflammation* 2013 **10**:57.